3 RESULTS

3.1 SPL3 expression in neuronal and non-neuronal tissue

SLP3 and stomatin are the closest homologues of MEC-2 in mammals. Using specific *slp3* mRNA probes all sensory neurones of the DRG and many neurones of the forebrain, hippocampus and spinal cord could be labelled by *in situ* hybridisation in mice (Wetzel et al., Nature 2006 in press).

In order to examine *slp3* expression in different adult mouse tissues in comparison to *stomatin* a quantitative Real Time PCR (qPCR) protocol was established to quantify the amount of *slp3* and *stomatin* mRNA transcripts. Using TaqMan Gene Expression Assays obtained from Applied Biosystems pre-designed primer and probe sets were chosen that correspond to the N-termini of *slp3* (TaqMan Expression Assay Mm00467671) and *stomatin* (TaqMan Expression Assay Mm00469130) because this region is quite divergent between the genes encoding both proteins.

Like human stomatin that is widely expressed in many tissues (Gallagher and Forget, 1995; Stewart et al., 1992) stomatin also seems to be ubiquitously expressed in mice. *stomatin* mRNA is present at similar levels in neuronal and non-neuronal tissues examined in this assay. Interestingly, *stomatin* mRNA is highly enriched in olfactory epithelium, where it is 1000-fold higher expressed than in any other tissue tested (Fig. 5).

slp3 mRNA on the other hand shows a much more specific expression pattern. It is present in DRG, brain and spinal cord but it is not detectable in any non-neuronal tissues examined apart from stomach. Similar to stomatin the expression level of *slp3* mRNA in olfactory epithelium is 1000-fold higher than in any other tissue examined, lower expression levels were found in DRG and brain.

Tissues with an overlapping expression of *stomatin* and *slp3* mRNA are: DRG, brain, spinal cord and both the olfactory bulb and the olfactory epithelium (Fig. 5).

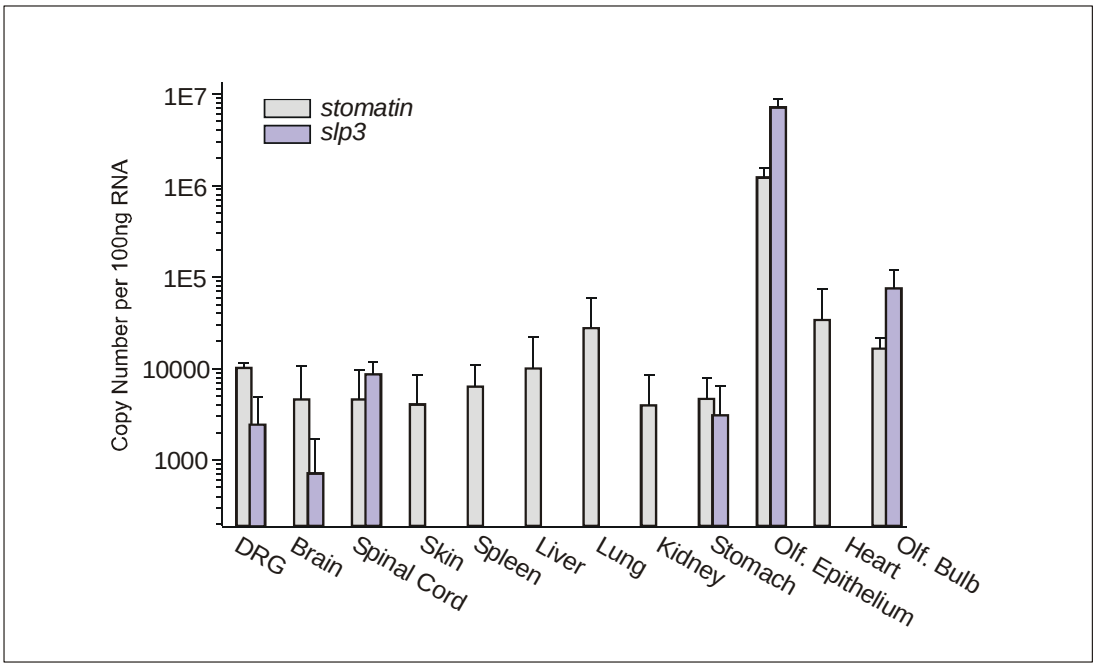

Figure 5 Expression of *stomatin* and *slp3* mRNA in various mouse tissues
Quantitative Real Time PCR (qPCR) was used to compare *stomatin* and *slp3* mRNA expression. cDNA preparations were made from neuronal and non-neuronal mouse tissues obtained from two mice (C5BL/6N) per qPCR run. Each run was repeated twice. For mRNA quantification, amplification rates of the target genes were normalised to threshold cycles determined for plasmids of known quantity containing either *slp3* or *stomatin* cDNA. *stomatin* mRNA is abundant in all tissues investigated, but like *slp3* mRNA it is highly enriched in olfactory epithelium. Note that *slp3* mRNA is more specifically expressed in the nervous system. Error bars indicate s.e.m.

3.2 Characterisation of SLP3$^{-/-}$ mice

Based on the specific expression of *slp3* mRNA in the nervous system including sensory neurones of the DRG, and because of the predicted secondary structure of the SLP3 protein that is highly similar to MEC-2 in *C. elegans*, SLP3 was considered to be a good mechanotransduction candidate molecule. A targeting construct (Fig. 6A) to mutate the *slp3* gene in mice was therefore made (Anne Mannsfeldt) in order to generate a new *slp3* mutant mouse line in collaboration with Dieter Riethmacher, ZMNH Hamburg.

3.2.1 Targeting of the slp3 locus in mice

In order to screen for positive ES-cell clones in which the targeting construct was successfully integrated by homologous recombination, a unique sequence within the genomic locus of *slp3* in mice was chosen to prepare a Southern blot probe complementary to a DNA sequence downstream of the short arm of the targeting construct. Using PCR oligonucleotide primers ("SLP3 probe up" and "SLP3 probe low") an amplification product of approximately 500bp was generated and subcloned in pGEM T-Easy. Subsequently, a P_{32} labelled RNA probe for *slp3* was generated and used in a radioactive genomic Southern blot on the F1 and F2 generation of the new *slp3* mutant mouse line (SLP3$^{-/-}$).

A ScaI restriction digest was used for analysis of mouse genomic tail DNA to reveal the targeted allele in SLP3$^{-/-}$ mice. As expected, a single DNA fragment was detected by the probe in homozygote mice, representing either wild-type (2.8 kb) or mutated alleles (3.5 kb) of the *slp3* gene. In heterozygotes the probe recognised two DNA fragments reflecting the existence of both alleles of the *slp3* gene (Fig. 6B).

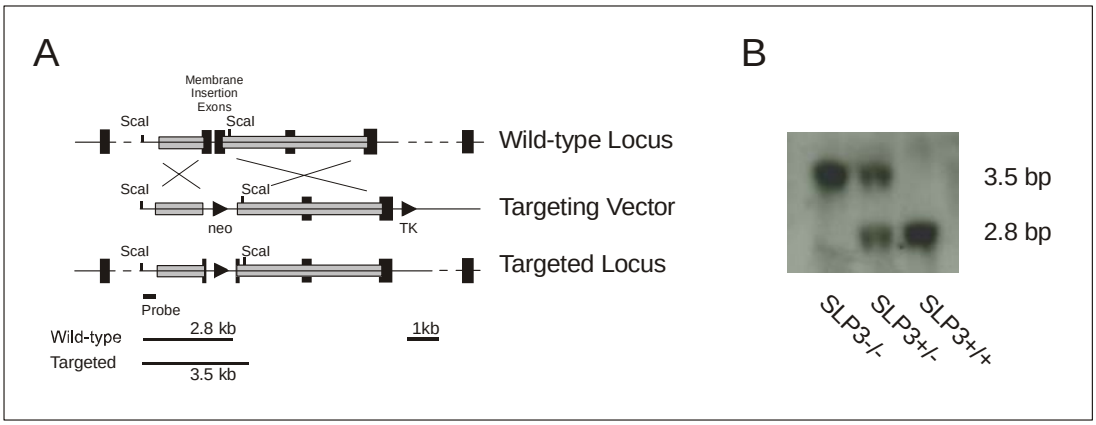

Figure 6 Southern blot hybridisation confirming the targeting mutation of the *slp3* gene in mice
A) Schematic diagram of the targeting strategy of the mutation inserted in the new *slp3* mutated mouse line is shown. A neomycin cassette replaces the membrane insertion domain encoded by exon 2-3 of the gene. ScaI restriction sites were used to reveal the targeted allele in a genomic Southern blot. The Southern blot probe is located downstream of the short arm of the targeting construct. **B)** Results from a typical Southern blot experiment following ScaI digestion of mouse $SLP3^{-/-}$, $SLP3^{+/-}$ or $SLP3^{+/+}$ tail DNA are shown. Genomic fragments detected by the radioactively labelled *slp3* probe represent either the wild-type (2.8kb) or the targeted allele of *slp3* (3.5kb).

3.2.2 $SLP3^{-/-}$ mice are healthy and viable

Homozygote *slp3* mutant mice are viable and fertile. Mating of *slp3* heterozygotes produced offspring as followed: 30% (15/50) wild-type homozygotes ($SLP^{+/+}$), 40% (20/50) heterozygotes ($SLP^{+/-}$) and 30% (15/50) homozygote mice deficient for SLP3 ($SLP3^{-/-}$). These results were statistically not different from the predicted Mendelian ratio (Chi-square test p=0.157). Body sizes and weights of $SLP3^{-/-}$ mice are not different compared to $SLP^{+/+}$ mice of the same age. Thus, disruption of the *slp3* gene in mice does not cause any profoundly gross physical or pathological manifestations. So far, the animals studied here apparently show no visible abnormalities in their postnatal development.

3.2.3 Genotyping of $SLP3^{-/-}$ mice

For genotyping $SLP3^{-/-}$ mice a PCR protocol was established using 5'prime oligonucleotides complementary to a unique sequence of the *slp3* gene downstream of the neomycin cassette in combination with 3'prime oligonucleotides

corresponding either to a unique sequence within the inserted neomycin cassette (SLP3$^{-/-}$ allele) or within exon 3 (SLP3$^{+/+}$ allele) (Fig. 7A).

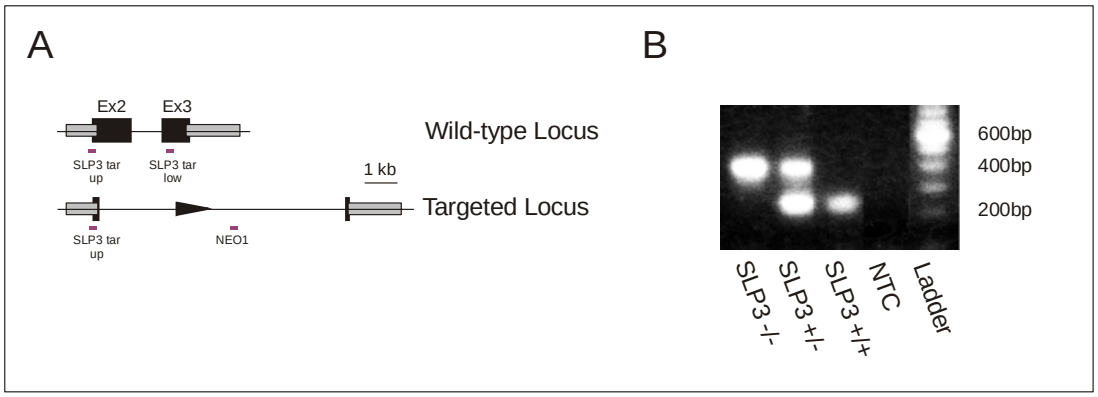

Figure 7 PCR strategy for determination of the genotype of wild-type or SLP3$^{-/-}$ mice
A) Oligonucleotide primer "SLP3 tar up" and "SLP3 tar low" were routinely used for amplifying a 250bp fragment from the wild-type genomic region including exons 2-3; a 400bp fragment derived from the mutated genomic locus was amplified using "SLP3 tar up" and "NEO1". **B)** A typical ethidiumbromide staining of the amplification products obtained from SLP3$^{-/-}$, SLP3$^{+/-}$ or SLP3$^{+/+}$ tail DNA is shown.

Figure 7B shows a typical ethidiumbromide staining of PCR amplification products obtained from SLP3$^{-/-}$, SLP3$^{+/-}$ or SLP3$^{+/+}$ genomic tail DNA. Whereas the larger band (400bp) detects specific PCR amplification products of the mutated allele of the *slp3* gene, the smaller band (250bp) is specific for the wild-type locus of *slp3* in mice.

3.2.4 Characterisation of SLP3$^{-/-}$ mice

The next step was to validate that the targeting of the *slp3* gene produces a null allele. cDNA was prepared from olfactory epithelium of SLP3$^{-/-}$ or SLP3$^{+/+}$ mice respectively. Several RT-PCR reactions were carried out using oligonucleotide primers as indicated in figure 8A: RT-PCR^{I} was used to test whether the neomycin cassette was successfully inserted into the wild-type locus during homologous recombination. Therefore, oligonucleotide primer "SLP3Ex1up" corresponding to a unique sequence following the start codon within exon 1 was combined with oligonucleotide primer "SLP3Ex3low" complementary to a unique sequence located within exon 3, which should have been replaced by the targeting event. To check

whether our *slp3* mutant mouse line could in principle also generate gene products resulting from a splicing event RT-PCR^{II} and RT-PCR^{III} were carried out.

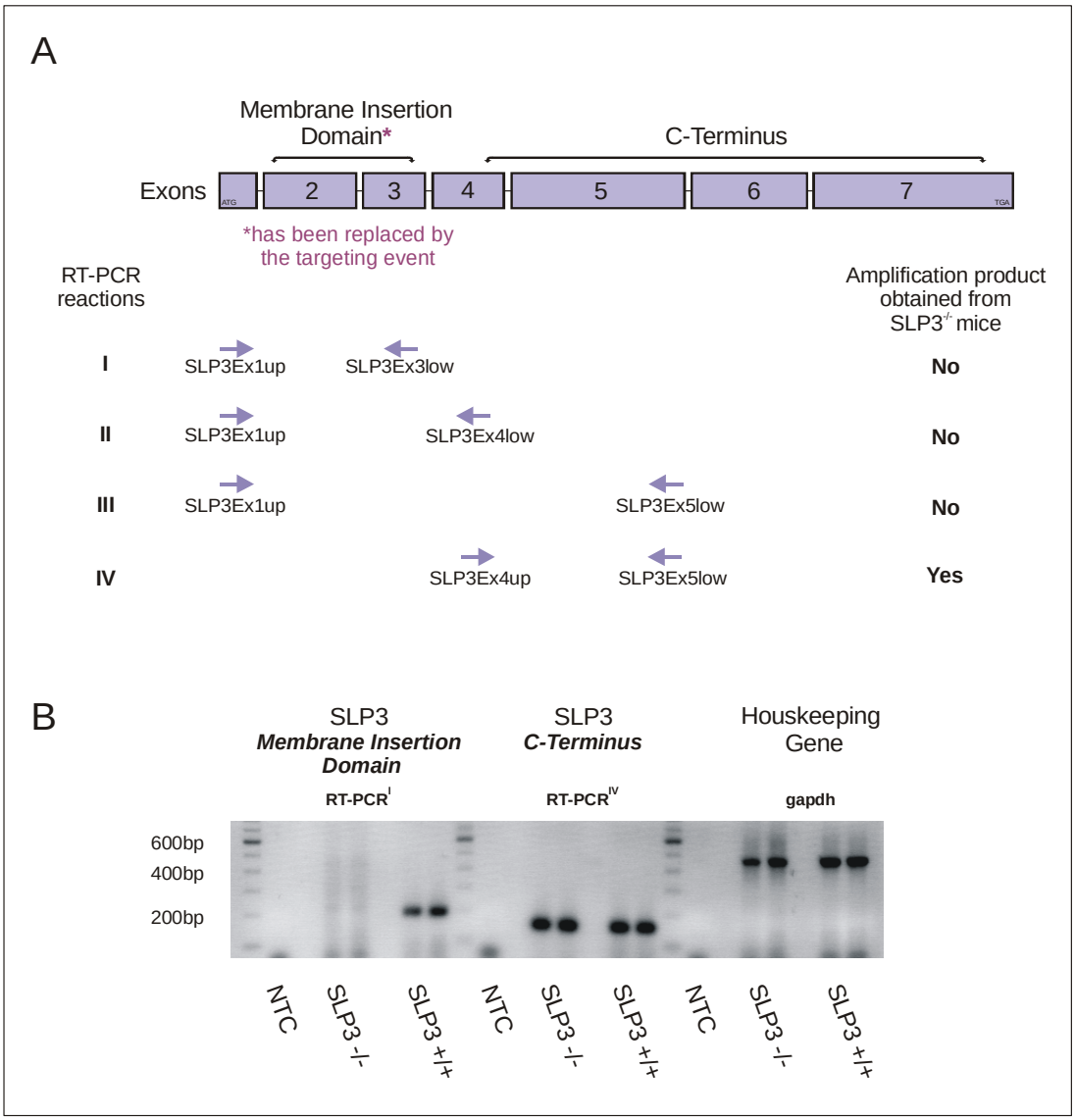

Figure 8 RT-PCR reactions carried out for further characterisation of SLP3$^{-/-}$ mice (mRNA level)

cDNA for all PCR reactions was prepared from olfactory epithelium. **A)** Oligonucleotide primers corresponding to unique sequences within the *slp3* gene were designed as indicated. RT-PCR $^{I-III}$ were carried out to control the targeting and/or eventually a splicing event, whereas RT-PCR ^{IV} was used to amplify a C-terminal product of the *slp3* gene. All RT-PCRs generated amplification products using cDNA obtained from wild-type mice. **B)** Oligonucleotide primers in RT-PCR^{I} amplified a 206bp PCR product in SLP3$^{+/+}$ mice but could not generate any amplification product in SLP3$^{-/-}$ mice. Oligonucleotide primers used in RT-PCR^{IV} generated a 153bp PCR product corresponding to the C-terminus of the *slp3* gene. This PCR product was amplified in both genotypes. Oligonucleotide primer pairs complementary to unique sequences within the housekeeping gene *gapdh* were carried out as control. All PCR reactions were performed in duplicates.

Thus, oligonucleotide primer “SLP3Ex1up” was combined with oligonucleotide primers “SLP3Ex4low” or “SLP3Ex5low” respectively. These primers were complementary to either a unique sequence within exon 4 or exon 5 of the *slp3* gene respectively. To address the possibility of the existence of an internal transcriptional promoter oligonucleotide primer pairs were designed that amplified the C-terminus of the *slp3* gene using the oligonucleotide primer pairs “SLP3Ex4up” and “SLP3Ex5low” (RT-PCR^{IV}).

All of the four RT-RCR reactions gave amplification products of the correct length and sequence using cDNA obtained from SLP3$^{+/+}$ mice. Using cDNA obtained from SLP3$^{-/-}$ mice no amplification products were generated when “SLP3Ex1up” and “SLP3Ex1low” were added to the reaction mixture (RT-PCR^{I}, Fig. 7B) confirming the targeting strategy that in the mutated alleles exon 2 and 3 have been successfully replaced during homologous recombination. Thus, our new transgenic mouse line is not able to generate a normal full-length transcript for the *slp3* gene.

No RT-PCR amplification products could be obtained from SLP3$^{-/-}$ animals using “SLP3Ex1up” in combination with either “SLP3Ex4low” or “SLP3Ex5low” respectively (RT-PCR^{II} and RT-PCR^{III}, data not shown) indicating that no splice variants of the *slp3* gene were produced by the mutated alleles. Since a C-terminal RT-PCR product of the gene could be amplified with the oligonucleotide primer pairs “SLP3Ex4up” and “SLP3Ex5low” (RT-PCR^{IV}, Fig. 8B) it is in principle still possible that an intrinsic transcriptional promoter exists within the genomic locus of *slp3* producing a truncated *slp3* transcript. All amplification products were subsequently subcloned in pGEM T-Easy and their inserts were subjected to DNA sequencing for product conformation.

3.3 Mechanosensory afferents in the skin require SLP3 for their function in mice

In order to test the involvement of SLP3 in sensory mechanotransduction in mice a series of electrophysiological studies were carried out using the *in vitro* skin nerve preparation (Koltzenburg et al., 1997; Reeh, 1988) to record from single sensory neurones in the saphenous nerve.

3.3.1 General aspects of the electrical and the mechanical search protocol used in the in vitro skin nerve preparation

The electrical search protocol is particularly suitable for discovering mechano-receptors that do not respond to mechanical stimulation (Kress et al., 1992). The starting point was the nerve trunk. By placing the stimulating electrode on top of the nerve, one to four single fibres were isolated in each filament and excited using supra threshold electrical stimuli. Based on the stability of the generated action potential and also on the heights of its amplitude, one or two units were chosen for further investigation. The action potential shape of a single unit was then monitored and both the electrical latency and conduction velocity of the unit were determined before tracing its axon peripherally by moving the electrode distally along the visible branching points of the nerve. Thereby the action potential shape of the unit was continuously monitored. The point where the recorded unit left the main nerve trunk presumably indicates the very close location where the axon branches to form its receptive field (RF) in the skin. Here the conduction velocity of the unit was measured again to make sure that it is still the same unit as at the start of the recording (Fig. 9 upper panel). The skin was then searched for a RF of the same unit by stimulating the skin with a blunt-end glass probe. Only units with identical action potential shape and conduction velocity for both electrical and mechanical search were tested for stimulus response function (Fig. 9 lower panel). In addition, these units must have had reproducible excitation by stimulation with the glass probe.

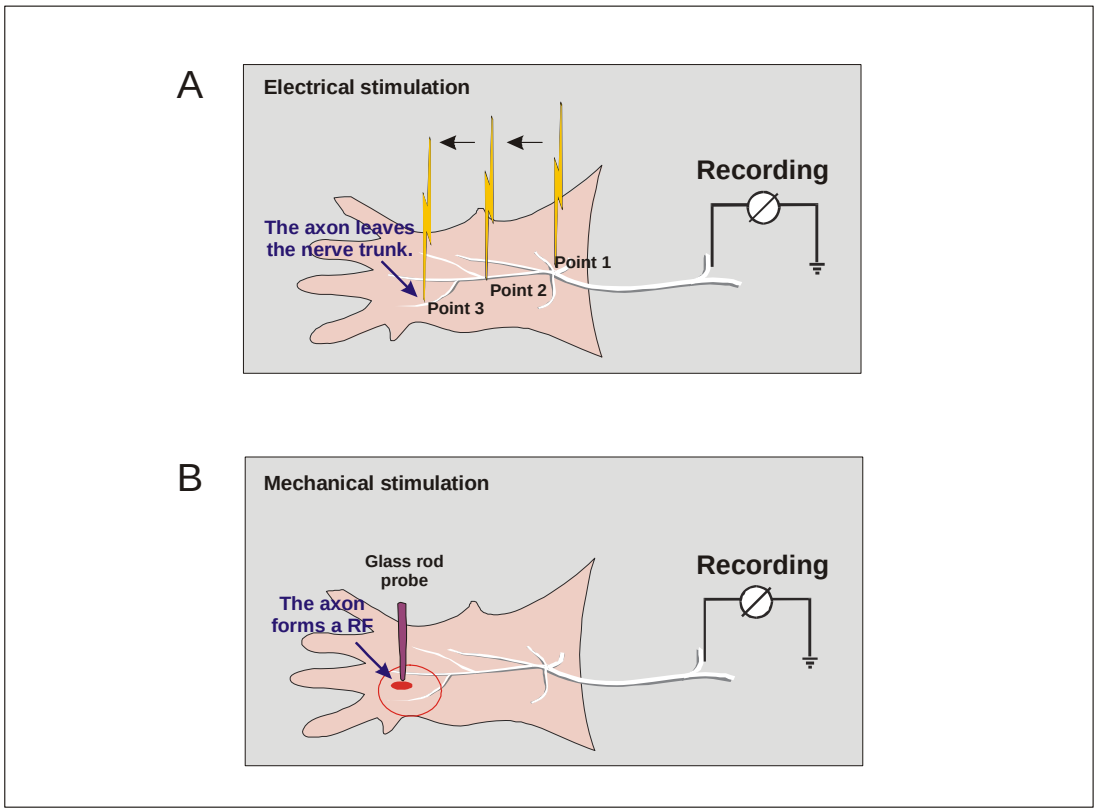

Figure 9 Electrical search protocol
The electrical search protocol illustrated here is particularly suitable for discovering mechano-insensitive receptors in the skin. Placing the stimulating electrode on top of the nerve trunk a single fibre is excited electrically at several points distally along the visible branching points of the nerve to follow the single unit in question (A). Around the point where its axon leaves the nerve trunk to form a receptive field in the periphery, the skin was searched mechanically for this unit using a blunt end glass rod (B). Thus, this experimental approach allows the experimenter to uncover those mechanoreceptors that lost their ability to detect mechanical stimuli.

The mechanical search protocol was particularly used to analyse individual mechanoreceptor types in more detail. Several parameters of the recorded units were examined: displacement stimulus responses function (Fig.10A), mechanical latencies (Fig.10C), von Frey thresholds and in addition in the case of low threshold mechanoreceptors (LTM) velocity stimulus response functions (Fig. 10B). Starting at the threshold for each unit, an ascending series of indentation stimuli was applied perpendicular onto the most sensitive point of the receptive field of the unit in question to obtain a stimulus response function. For data analysis, the average firing rate (spikes/sec) during a ten second mechanical stimulation was determined and plotted for each displacement. Since rapidly-adapting mechanoreceptors respond exclusively to the ramp phase of a mechanical stimulus, a special stimulation

protocol was used to investigate how the fibres' firing rates vary with different velocities of the movement.

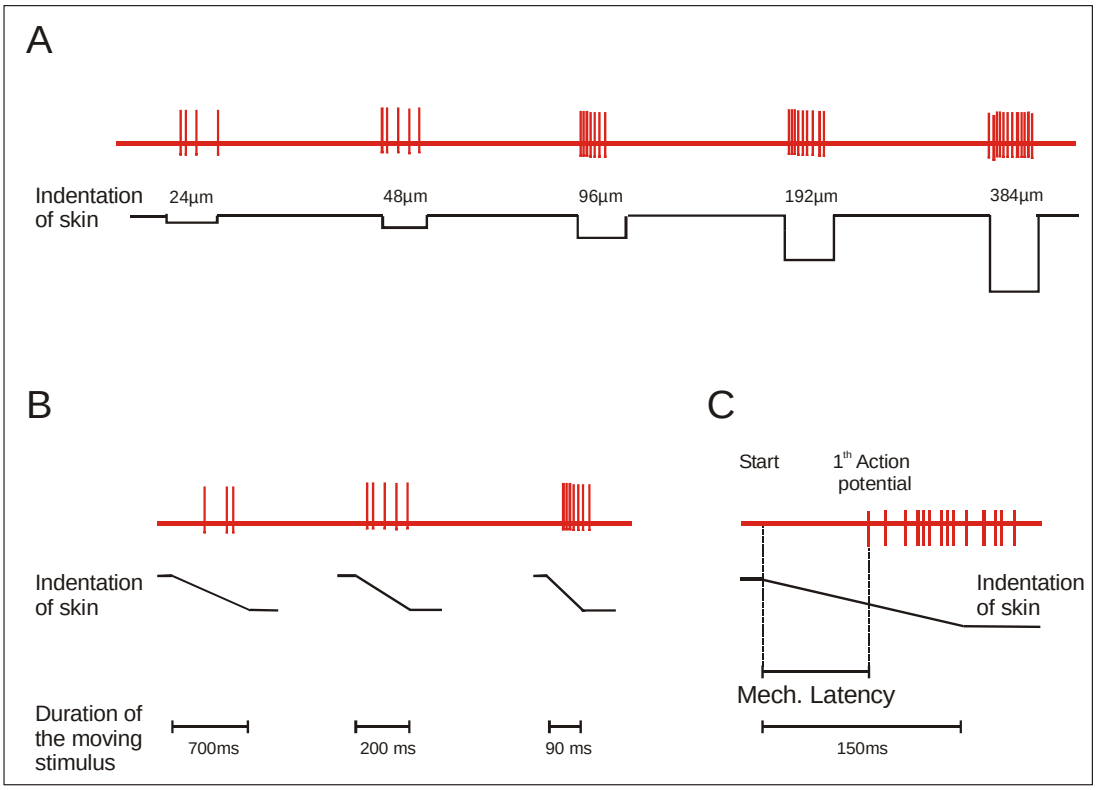

Figure 10 Schematic drawing of mechanical parameters studied using the mechanical search protocol
Mechanical parameters analysed for evaluating mechanoreceptor function in mice are illustrated: **A)** The stimulus response function is produced by an ascending series of increasing displacement stimuli. **B)** The velocity response function is generated following application of varying movement velocities. **C)** The mechanical latency reflects the time interval from the onset of a mechanical stimulus until the first action potential is fired.

The mechanical latency gives information about the time interval from the onset of the mechanical stimulus until the first action potential is fired (Fig. 10C). Thus, mechanical latency is a reflection of the time a mechanotransducer needs to convert a mechanical signal into an action potential. This timing varies with displacement strength and velocity of the movement.

Table 1 and 2 below give an overview of the total number of units that were isolated from the saphenous nerve for recordings in the skin nerve preparation using the electrical search (Table 1) or the mechanical search protocol (Table 2).

	SLP3 $^{+/+}$ (electrical search)		**SLP3 $^{-/-}$ (electrical search)**	
Receptor Type	**Number**	**% Total**	**Number**	**% Total**
Aβ-Fibres Aβ- units	50		101	
no RF	4	8.0	39	38.6
Aδ-Fibres Aδ- units	18		68	
no RF	1	5.6	22	32.4
C-Fibres C- units	20		17	
no RF	2	10.0	1	5.9

Table 1 Detailed breakdown of the single fibre recordings from SLP3$^{-/-}$ and SLP3$^{+/+}$ mice using the electrical search protocol
Data that are shown here were obtained from the electrical search protocol. Note that mechano-insensitive fibres found in SLP3$^{-/-}$ or SLP3$^{+/+}$ mice are displayed as no receptive field units (no RF).

	SLP3 $^{+/+}$ (mechanical search)			**SLP3 $^{-/-}$ (mechanical search)**		
Receptor Type	**% Total**	**CV m/s**	**vFT**	**% Total**	**CV m/s**	**vFT**
Aβ-Fibres RAM	40.7 (22/54)	13.8±0.62	1.0 (0.4/6.3)	44.4 (20/45)	15.7±0.64	1.4 (0.4/10)
SAM	59.3 (32/54)	13.8±0.64	1.4 (0.4/13.0)	55.6 (25/45)	14.8±0.52	2.0 (0.4/13)
Aδ-Fibres AM	70.5 (31/44)	5.3±0.44	2.0 (1.0/13.0)	63.3 (19/30)	6.05±0.51	6.3 (1.0/13.0)
D-hair	29.5 (13/44)	4.5±0.51	0.4	36.7 (11/30)	4.3±0.44	0.4 (0.4/1.0)
C-Fibres C-units	(35)	0.53±0.03	10.0 (2.0-47.0)	(37)	0.55±0.04	6.3 (1.4-24.0)
C-M	37 (10/27)	0.62±0.07	6.3 (2.0-10.0)	31.6 (6/19)	0.64±0.09	6.3 (6.3-10.0)
C-MH	63 (17/27)	0.74±0.03	13.0 (3.3-22.0)	68.4 (13/19)	0.41±0.02	10.0 (1.4-24.0)

Table 2 Detailed breakdown of the single fibre recording from SLP3$^{-/-}$ and SLP3$^{+/+}$ mice using the mechanical search protocol
Receptor proportions (% Total), conduction velocities (CV) and mechanical thresholds (vFT) are shown for individual mechanoreceptor classes. Note that no parameter was found to be significantly different between SLP3$^{+/+}$ and SLP3$^{-/-}$ mice. Median values are shown with the 1st and 3rd quartile range. Means are expressed as ± s.e.m.

3.3.2 A-fibre mechanoreceptors lose mechanosensitivity in SLP3$^{-/-}$ mice

In order to test whether SLP3$^{-/-}$ mice show a selective loss of sensory afferents in the skin the electrical search protocol was applied to 248 single fibres derived from 31 adult (>6 weeks) SLP3$^{-/-}$ mice. Ninety-five single fibres obtained from 18 SLP3$^{+/+}$ animals were studied in the same way. The analysis was done blind, i.e. the genotype of the mouse was not revealed until after a series of experiments were completed.

Using this methodology in SLP3$^{+/+}$ mice most of the fibres studied were mechanically sensitive, i.e. 46 of 50 Aβ-fibres, 17 of 18 Aδ-fibres and 18 of 20 C-fibres that were driven electrically on the nerve had a mechanosensitive RF in the skin. Thus, less than 10% of the recorded A-fibres as well as C-fibres could only be driven electrically, i.e. no RF in the skin was found for these fibres (Fig. 11B).

In marked contrast to these findings, a drastic reduction in the number of mechanically responsive fibres was observed in SLP3$^{-/-}$ mice (Fig. 10B). Approximately 36 % (39 of 101) of Aβ- and 30% (22 of 68) of Aδ-fibres studied using the electrical approach were not found to have a RF in the periphery and these proportional changes were statistically significant in both cases (Chi-square test $p<0.001$ (Aβ), $p=0.022$ (Aδ)). Note that immediately after mechanical search for a RF of a fibre the nerve trunk was electrically stimulated again to confirm the integrity of the fibre. Only those fibres, which still could be electrically excited, were regarded as mechano-insensitive (Fig. 11A, B). The location of RFs of single sensory afferents in the skin were randomly distributed over the entire innervation territory of the saphenous nerve in SLP3$^{+/+}$ as well as in SLP3$^{-/-}$ mice and mostly found slightly distal to the last point from which the electrical stimulation of the nerve trunk was successful. In contrast to the loss of mechanosensitivity in A-fibres no changes were observed in C-fibres. In SLP3$^{+/+}$ mice, 2 of 20 fibres (10%) did not possess a mechanosensitive RF in the skin and 1 of 17 fibres could not be assigned to a RF in the periphery in SLP3$^{-/-}$ mice (Chi-square test $p=0.647$, Fig. 11B)).

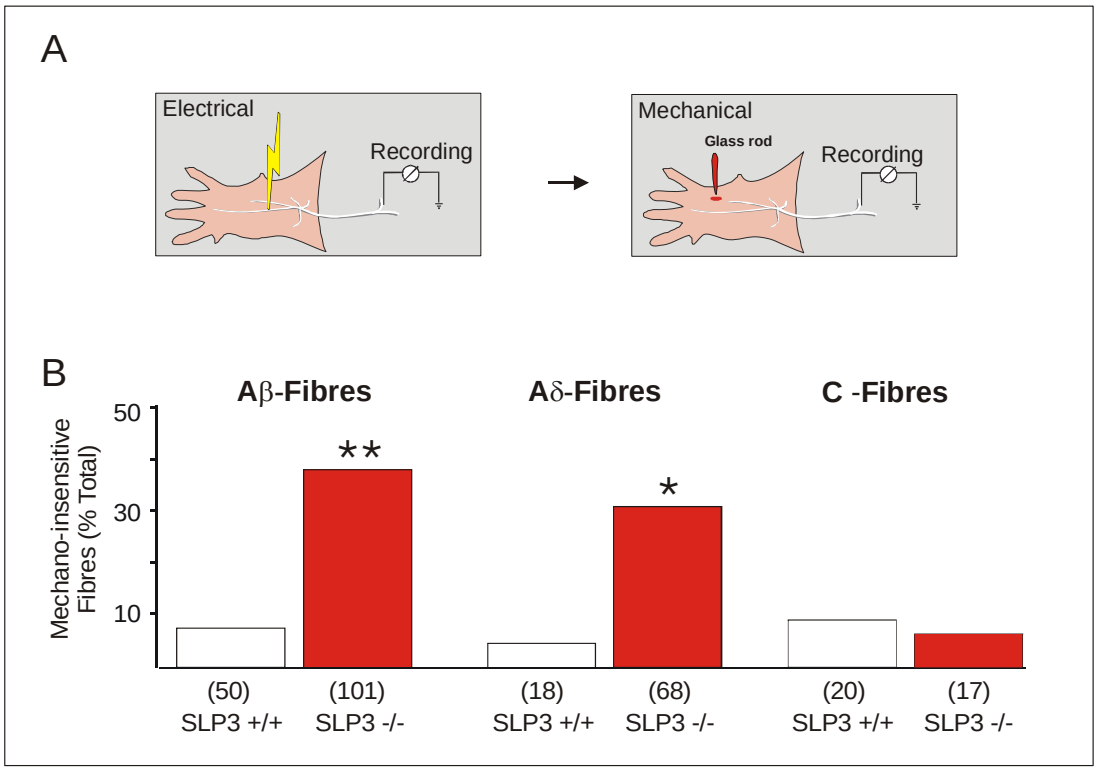

Figure 11 Mechanically insensitive sensory afferents in SLP3$^{-/-}$ mice
A) The electrical search protocol was used. Singe fibres were isolated by electrical stimulation of the nerve prior to searching for a RF of the same fibre in the periphery using a mechanical search stimulus (blunt end glass rod). **B)** In SLP3$^{+/+}$ mice less than 10% of all fibres classified lack a mechanosensitive RF, but in marked contrast to controls 30-40% of all A-fibres identified by electrical stimulation lack mechanosensitivity in SLP3$^{-/-}$ mice (Chi-square test **p<0.005 *p<0.05). Note that the proportion of mechano-insensitive C-fibres was unchanged (Chi-square test p>0.05). The numbers of single neurones recorded in each category are indicated below each column.

Since mechano-insensitive fibres, found using the electrical search stimulus, could not be by definition classified as belonging to any mechanoreceptor class a mechanical search protocol (for detailed information see also methods) was used to investigate mechanoreceptor incidences in SLP3$^{-/-}$ mice. A-fibres can be divided into four major types, of which three are low threshold mechanoreceptors (LTM) that can further be subclassified into rapidly-adapting (RAM) or slowly-adapting (SAM) mechanoreceptors of the Aβ-type and D-hairs of the Aδ-type. A-fibre mechanonociceptors (AM), the fourth type, are high threshold mechanoreceptors (HTM) conducting in the Aδ-range. Therefore, stimulus response functions were recorded from 98 A-fibres obtained from 13 SLP3$^{+/+}$ mice and from 57 A-fibres isolated from 8 SLP3$^{-/-}$ mice.

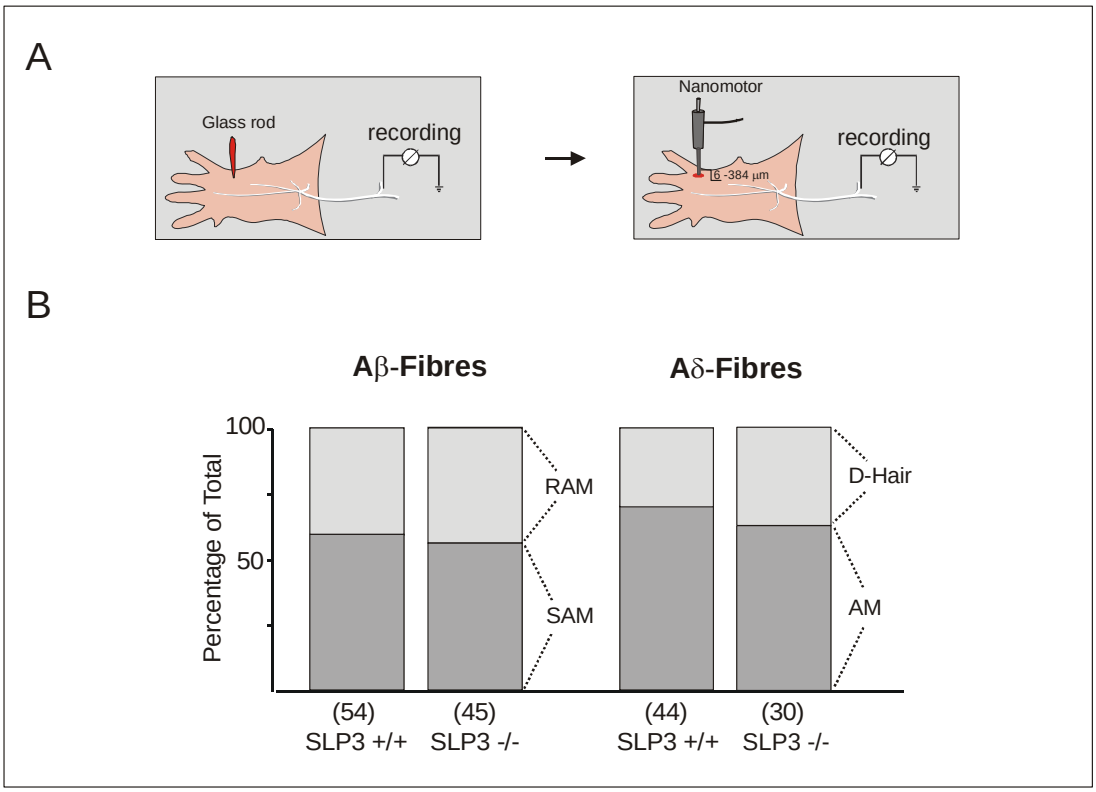

Figure 12 Proportion of mechanosensitive A-fibre afferents in SLP3$^{-/-}$ mice
A) The mechanical search protocol is shown. **B)** The receptor proportion of fast conducting Aβ-fibres that can be classified as RAM or SAM was not changed in SLP3$^{-/-}$ mice compared to wild-type littermates (Chi-square test $p>0.05$). There was also no proportional change observed in Aδ-fibres classified as D-Hair or AM (Chi-square test $p>0.05$). The number of single fibres recorded in each category is indicated below each column.

In SLP3$^{+/+}$ mice 40.7% (22 of 54) of the mechanoreceptors were classified as RAM and 59.3% (32 of 54) as SAM amongst the Aβ-fibres. In the Aδ-range, 70.5% (31 of 44) exhibited AM properties and 29.5% (13 of 44) were D-hairs. A conspicuous change in A-fibre receptor distribution should be observed in SLP3$^{-/-}$ mice if any single mechanoreceptor class is selectively affected by the mutation. Surprisingly, the proportions of neither the fast conducting Aβ-fibres, of which 44.4% (20 of 45) were classified as RAM and 55.6% (25 of 45) as SAM, nor the proportion of the slowly conducting Aδ-fibres composed of 63.3% (19 of 30) AM and 36.7% (11 of 30) D-hairs were changed in SLP3$^{-/-}$ mice compared to wild-type littermates (Chi-square test $p=0.710$ (Aβ), $p=0.52$ (Aδ), Fig.12B).

Thus, no apparent loss of mechanoreceptors in a specific receptor type could be inferred from the relative incidence of the A-type mechanoreceptor classes in SLP3$^{-/-}$ mice.

3.3.3 Electrical thresholds of mechano-insensitive A-fibres are unchanged in SLP3$^{-/-}$ mice

In order to test whether the *slp3* mutation could adversely affect or alter electrical excitability of mechanically insensitive sensory neurones control experiments were carried out. The electrical search protocol was applied to 31 additional A-fibres isolated from 3 SLP3$^{-/-}$ mice. The electrical stimulation strength needed to evoke an action potential was measured from the nerve trunk and electrical thresholds of mechano-insensitive A-fibres were compared to electrical thresholds of A-fibres that formed a functional RF in the skin. The results indicate that there is no difference in electrical threshold observed for mechano-insensitive or mechanosensitive fibres in SLP3$^{-/-}$ mice (Aβ-fibres: I_{MIS}=4.85mA, I_{MS}=5.43; pulse duration=50µs; Aδ-fibres: I_{MIS}=5mA, I_{MS}=5.69; pulse duration=150µs) (unpaired T-test p=0.504 (Aβ), p=0.574 (Aδ), Fig. 13).

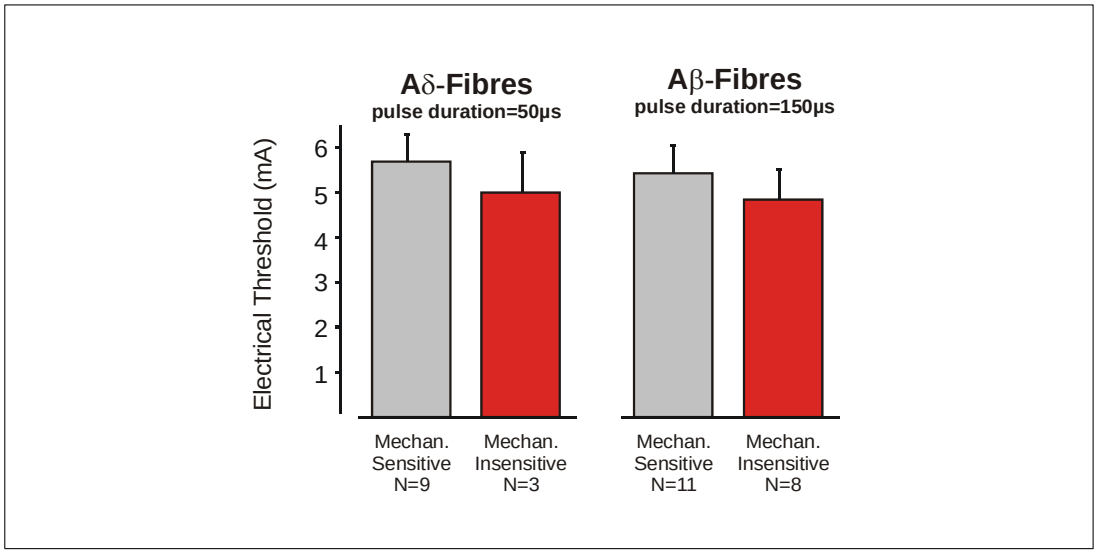

Figure 13 Electrical thresholds of mechano-insensitive fibres in SLP3$^{-/-}$ mice
Electrical currents were applied to the nerve trunk in order to excite single fibres that exhibited either mechano-insensitive or mechanosensitive properties. Electrical thresholds that evoked action potentials in these fibres were determined to compare electrical excitability of mechano-insensitive and mechanosensitive A-fibres in SLP3$^{-/-}$ mice. Note that there is no difference in electrical excitability observed for mechano-insensitive and mechanosensitive fibres in SLP3$^{-/-}$ mice (unpaired T-test p>0.05). Error bars indicate s.e.m.

3.3.4 Mechanoreceptor function is impaired in SLP3$^{-/-}$ mice

Over a third of the myelinated sensory afferents in the skin of SLP3$^{-/-}$ mice were found to be mechano-insensitive. Therefore, the coding ability of the remaining functional A- and C-fibres was systematically examined with a range of quantitative mechanical stimuli.

Starting at threshold for each single mechanoreceptor a series of displacement stimuli was applied perpendicularly to the most sensitive point of the RF. Stimuli rose from 6µm to 384µm in the case of LTM or from 12µm to 768µm for HTM (Fig. 14). In some experiments heat stimuli were applied to C-fibre mechanoreceptors.

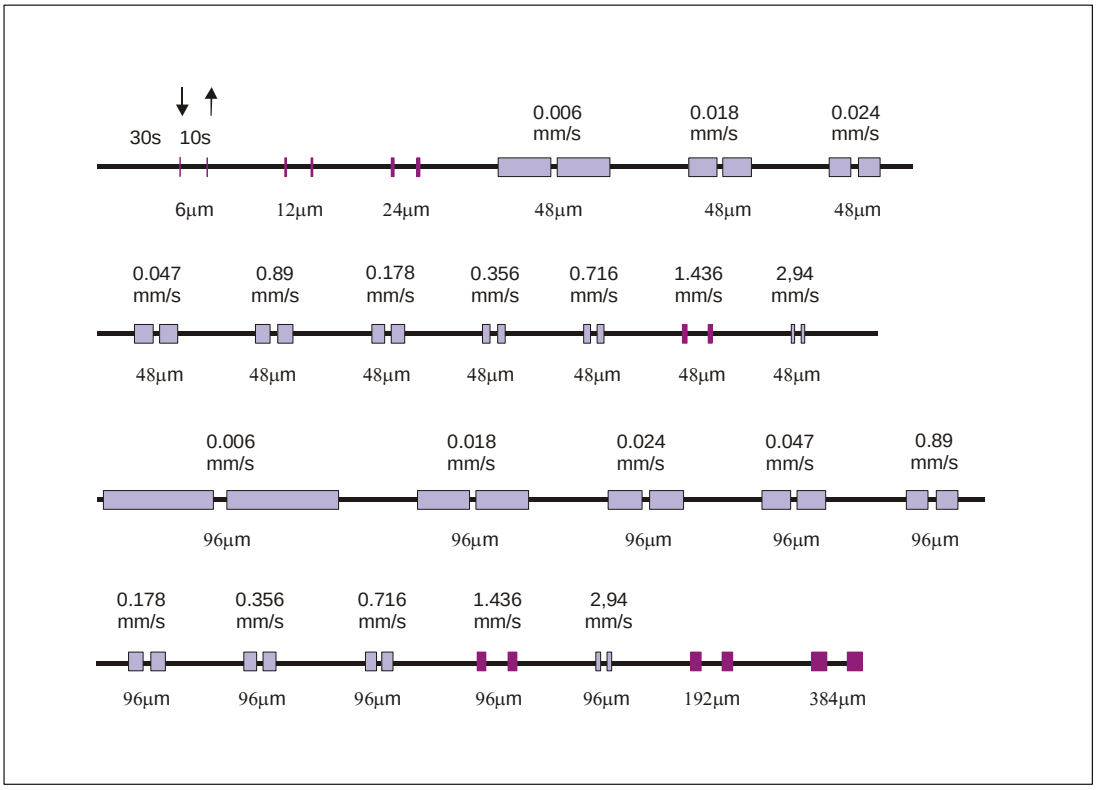

Figure 14 Mechanical stimulation protocol for studying mechanoreceptor properties in the skin
The mechanical stimulation program for generating a stimulus response and velocity response function in single sensory afferents in the skin is shown. The series of displacement stimuli starts at 6µm and stimuli usually rise up to 384µm (purple square) and in between two series of velocity stimuli (5.9 to 2942 µm/sec) are included at two constant displacements (48µm and 96µm, pastel blue square).

For low threshold mechanoreceptors, the stimulation protocol was combined with variable velocity stimuli (5.9 to 2942 µm/sec) at two constant displacements (48µm

and 96µm). The 96µm displacement was chosen for velocity analyses since this displacement produced more reliable results at lower velocities than varying velocity stimulations applied to the skin at the 48µm displacement (Fig. 14).
Using this methodology recordings were made from 85 fibres obtained from SLP3$^{-/-}$ mice and 133 fibres isolated from wild-type littermates. Stimulus and velocity response functions or mechanical latencies were analysed separately for each mechanoreceptor subclass.

3.3.4.1 Mechanosensitivity of RAM fibres in SLP3$^{-/-}$ mice

In the hairy skin RAM fibres can be assigned to hair follicle receptors such as lanceolate and pilo-Ruffini endings, field receptors or Pacinian corpuscles (Brown, 1967; Burgess and Perl, 1967). Using the *in vitro* skin nerve preparation we are not able to record from Pacinian corpuscles, as they are located deep in subcutaneous tissue in rodents (Burgess, 1968; Lewin and McMahon, 1991).
When the coding ability of these fibres was examined in detail it was found that 45% (9 of 20) of all RAM fibres tested could not be stimulated by the fastest movement (2.9mm/sec) produced by the nanomotor. Since tapping of the receptive field with the glass rod probe was the only possibility to excite these fibres, they were classified as “tap” units. Interestingly, these “tap” units, which therefore responded to mechanical stimulation only when the stimulus was very rapidly applied to the skin made up only 4.5% (1 of 22) in SLP3$^{+/+}$ mice. The increase in the proportion of RAM fibres in SLP3$^{-/-}$ mice with a “tap” response was highly statistically significant (Chi-square test $p<0.0027$, Fig. 15A).
The conduction velocities of the “tap” units (15.8 ±0.8 m/s) in SLP3$^{-/-}$ mice were not different from the remaining functional “non-tap” RAMs (15.7 ±1.0 m/s) in these mutants (unpaired T-test $p=0.93$). Von Frey thresholds of the “tap” units in SLP3$^{-/-}$ mice on the other hand were slightly increased. “Tap” units were excited by mean forces of 2.0mN (n=9, median value), whereas the mean force needed to excite the remaining “non-tap” RAMs in SLP3$^{-/-}$ mice was 1.0mN (n=9, median value). However, these differences did not reach statistical significance (Mann-Whitney U-test $p=0.108$).

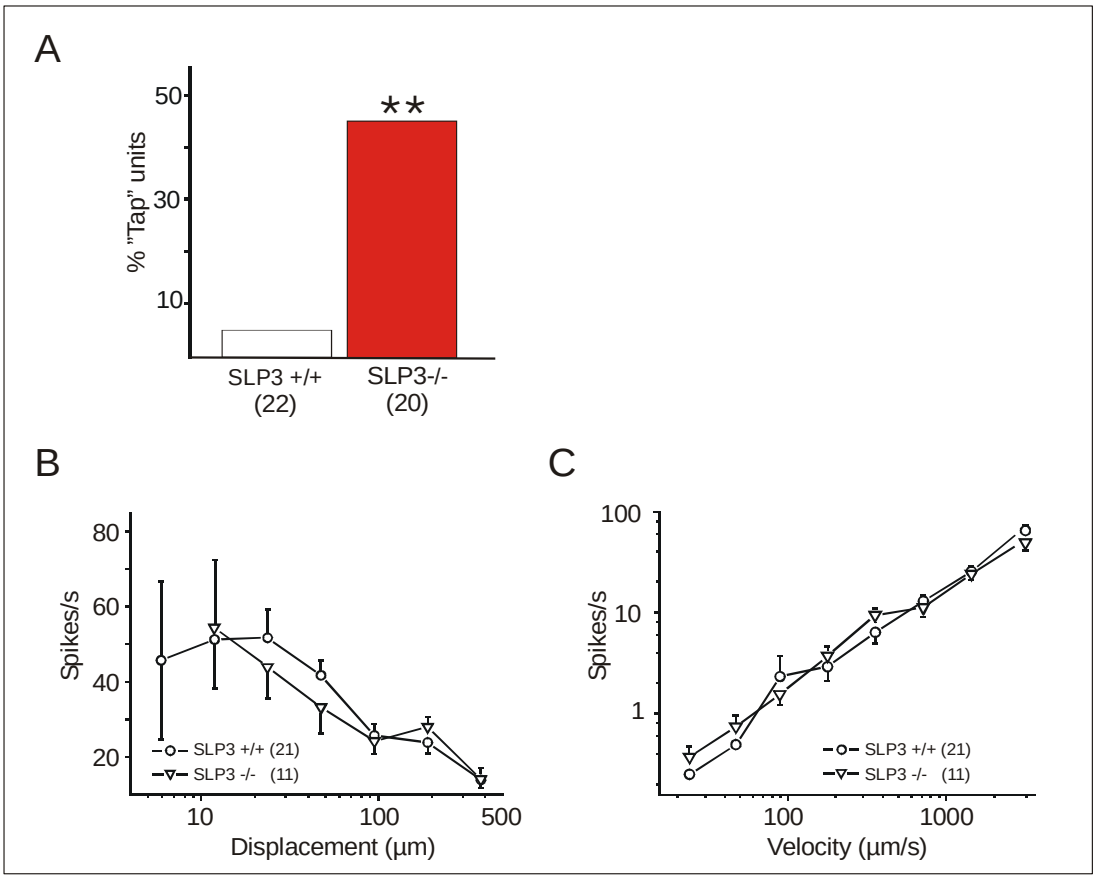

Figure 15 Mechanosensitivity of RAM fibres in SLP3$^{-/-}$ mice
A) The proportion of RAM fibres that responded with a so-called "tap" response was significantly greater in SLP3$^{-/-}$ mice (Chi-square test **p<0.005). **B, C)** Mechanoreceptor firing rates during the movement phase of the mechanical stimulation are plotted against increasing displacement amplitude **(B)** or velocity **(C).** Note that displacement as well as velocity sensitivity was not significantly changed in SLP3$^{-/-}$ compared to SLP3$^{+/+}$ mice (repeated measures ANOVA p>0.05). Error bars indicate s.e.m.

Rapidly-adapting mechanoreceptors show marked responses exclusively to the dynamic phase of a ramp and hold mechanical stimulation. Responses to the movement phase of distinct displacement stimuli (6µm to 368µm) were analysed for the remaining eleven "non-tap" RAM fibres obtained from SLP3$^{-/-}$ mice. No substantial deficit in the mechanosensitivity of these fibres was found when their coding ability was compared to RAM fibres from SLP3$^{+/+}$ mice (repeated measures ANOVA $F_{(1.25)}$ =0.723, p=0.403, Fig. 15B). The velocity response function of RAM fibres from SLP3$^{-/-}$ mice, produced at 96µm displacement, was essentially identical to that seen in wild-type littermates (repeated measures ANOVA p=0.056, Fig. 15C).

3.3.4.2 Mechanosensitivity of SAM fibres in SLP3$^{-/-}$ mice

There are two major receptor types in mice classified as slowly-adapting mechanoreceptors: Type II or SA-2 receptors (Chambers and Iggo, 1967) typically show a regular firing pattern and the firing frequency increases with displacement strength of the mechanical stimulation (Burgess, 1968; Chambers et al., 1972; Perl, 1968). Type I or SA-1 fibres show robust responses to the movement phase of ramp and hold stimuli of a mechanical stimulation. These fibres generate action potentials with a less regular firing pattern compared to SA-2 during sustained indentation of the skin (Perl, 1968; Pubols, 1990). Most SAM fibres recorded here presumably resembled SA-1 mechanoreceptors that innervate Merkel cell complexes of touch domes (Airaksinen et al., 1996; Iggo and Andres, 1982; Iggo and Muir, 1969; Koltzenburg et al., 1997).

Twenty SAM fibres isolated from SLP3$^{-/-}$ mice and 24 SAM fibres identified in SLP3$^{+/+}$ mice were tested for stimulus and velocity response function.

In SLP3$^{-/-}$ mice the firing frequency of SAM fibres at lower displacements (6µm–24µm) was similar to that seen in control units obtained from SLP3$^{+/+}$ mice. At higher displacements (48µm-384µm) a rightward shift of the stimulus response function indicating that SAM fibres in SLP3$^{-/-}$ mice were less mechanosensitive was observed. This reached statistical significance at 96µm (unpaired T-test p=0.043, Fig. 16A left). Mechanical latencies of SAM fibres in SLP3$^{-/-}$ mice were not statistically different when compared to SAM fibres from SLP3$^{+/+}$ mice (repeated measures ANOVA $F_{(6.36)}$=1.24 p=0.31, Fig. 16A right).

The ability for coding the stimulus velocity of a mechanical stimulation was also reduced in SLP3$^{-/-}$ mice, an effect that was prominent at almost all movement velocities. However, the difference in firing rate during the movement phase was statistically significant only when a velocity stimulus of 178µm/sec was applied at 96µm displacement (unpaired T-test p=0.04, Fig. 16B left). Mechanical thresholds were slightly but statistically significantly altered at several velocities, i.e. in SLP3$^{-/-}$ mice an increase in mechanical latency was observed at 89µm/sec to 716µm/sec stimulus velocity compared to controls (unpaired T-test p=0.023 (89µm/sec), p=0.004 (179µm/sec), p=0.03 (359µm/sec), p=0.047 (716µm/sec), Fig. 16 right).

Thus, the coding ability of a mechanical stimulation as well as the stimulus velocity needed to evoke threshold responses in SAM fibres appears to be affected by loss of SLP3 in mice.

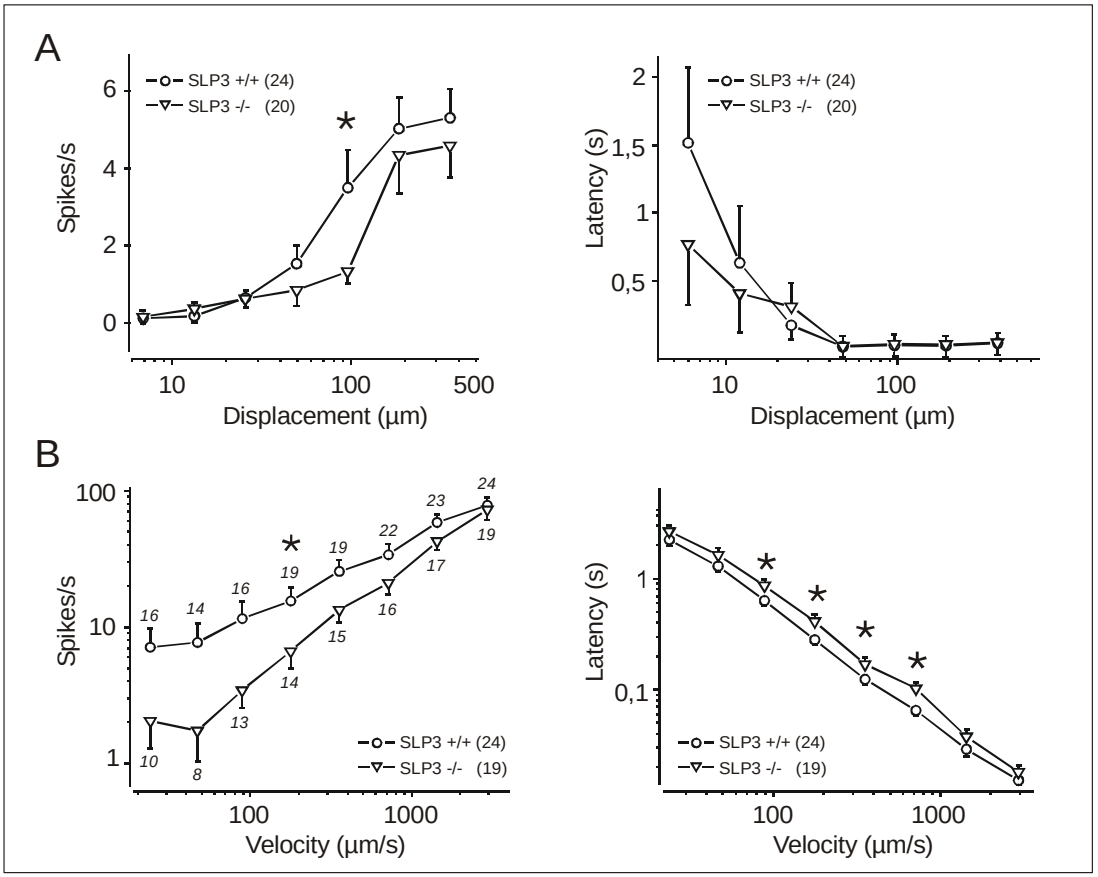

Figure 16 Mechanosensitivity of SAM fibres in SLP3$^{-/-}$ mice
Displacement (upper panel) and velocity (lower panel) protocols were used to produce a stimulus response function in SAM fibres in SLP3$^{+/+}$ and SLP3$^{-/-}$ mice. Mechanical latencies were also measured (right panel). **A)** SAM fibres from SLP3$^{-/-}$ mice appeared to be less sensitive at indentations above 24µm and this was significantly different at 96µm (unpaired T-test *p<0.05), but mechanical latencies were unchanged (repeated measures ANOVA p>0.05). **B)** The mechanical coding ability of the movement velocity (stimulus intensity was 96µm) was affected in SLP3$^{-/-}$ mice and this reached statistical significance (unpaired T-test *p<0.05) where indicated. Error bars reflect the s.e.m.

3.3.4.3 Mechanosensitivity of D-hairs in SLP3$^{-/-}$ mice

D-hair receptors are velocity detectors most effectively excited by movements of hairs or of the skin surface (Adriaensen et al., 1983; Burgess and Perl, 1967; Dubreuil et al., 2004; Koltzenburg et al., 1997; Lewin and McMahon, 1991; Lewin et

al., 1992b; Perl, 1968). However, there is no clear data published identifying the morphology of D-hairs, but it seems likely that they are associated with hairs (Stucky et al., 1998).

Recordings were made from 9 D-hairs in SLP3$^{-/-}$ and 11 D-hairs in SLP3$^{+/+}$ mice. Since D-hairs exclusively respond to the dynamic phase of a mechanical stimulation, the firing rate during the movement to changing displacements was analysed. In SLP3$^{-/-}$ mice a slight, but not statistically significant, reduction of the firing rate was observed when larger displacement stimuli (96µm- 384µm) were applied to the skin (repeated measures ANOVA $F_{(2.46)}$ =0.478, p=0.08, Fig. 17A left). Mechanical latencies determined for the different displacement stimuli were not altered in SLP3$^{-/-}$ mice compared to wild-type littermates (repeated measures ANOVA F= $_{(5.2)}$= 1.41 p=0.26, Fig.17A right).

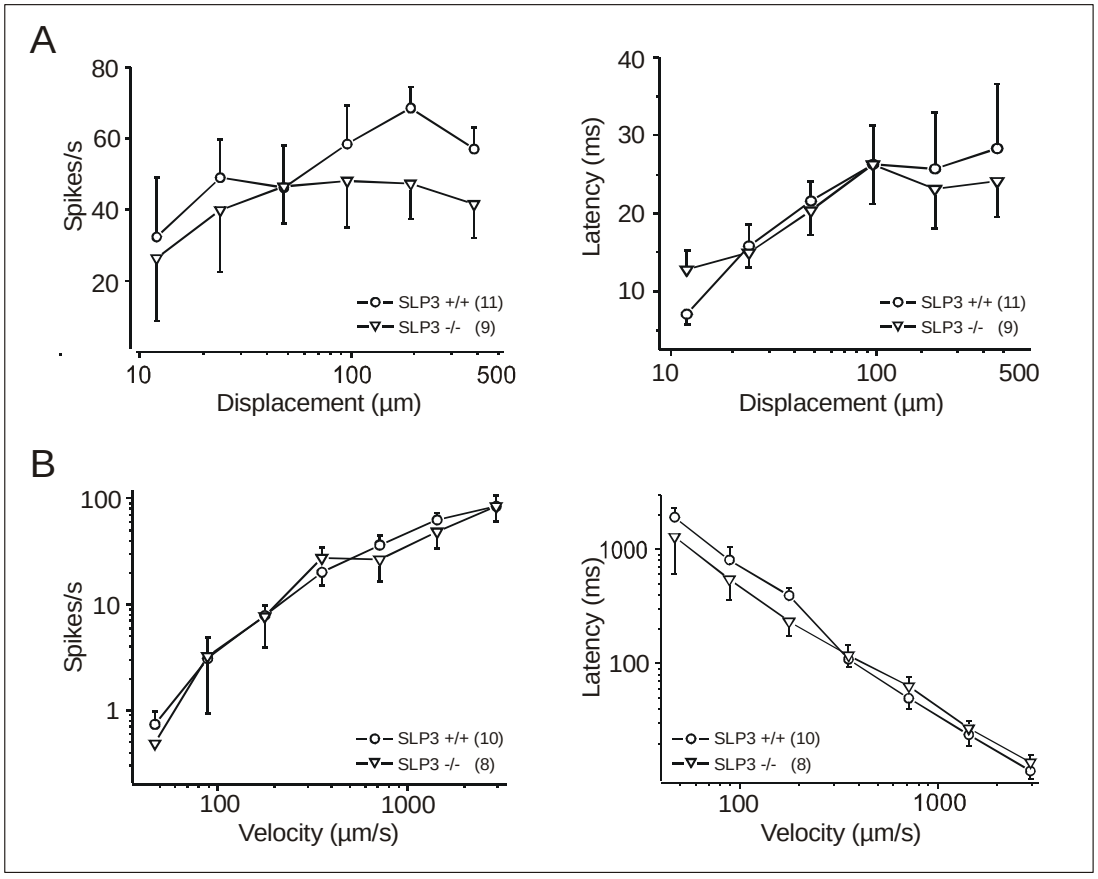

Figure 17 Mechanosensitivity of D-hairs in SLP3$^{-/-}$ mice
Displacement **A)** and velocity **B)** protocols were used. Stimulus response functions (left panel) and mechanical latencies (right panel) were analysed for an ascending series of indentation or velocity stimuli. No significant differences were observed for any parameters analysed for D-hairs obtained from SLP3$^{-/-}$ or SLP3$^{+/+}$ mice (repeated measures ANOVA p>0.05). Error bars indicate s.e.m.

In terms of velocity sensitivity, which is best coded by D-hair receptors, no difference in stimulus response function to varying ramp velocities was found in SLP3$^{-/-}$ mice compared to wild-type littermates (Fig.17B left). The latency for the first spike mechanically evoked by varying velocities of the movement is plotted in Fig 17B (right) indicating that the indentation needed to elicit threshold response is not different between D-hairs in both genotypes (repeated measures ANOVA $F_{(6.1)}$= 2.56 p=0.078).

3.3.4.4 Mechanosensitivity of AM fibres in SLP3$^{-/-}$ mice

Nociceptors possess either Aδ- or C-fibre afferent axons. In the case of AM fibres they have thinly myelinated axons and almost form certainly “free nerve endings” associated with Schwann cells or keratinocytes in the epidermis (Kruger et al., 1981). The coding ability of 15 (SLP3$^{-/-}$) and 28 (SLP3$^{+/+}$) AM fibres was examined by applying displacement stimuli ranging from 12µm to 768µm in amplitude. Action potentials evoked during the ten second displacement stimulation were averaged for each displacement and plotted as action potentials per second in a stimulus response function, but AM fibres from SLP3$^{-/-}$ mice did not show any alteration in their mechanosensitivity when compared to SLP3$^{+/+}$ mice (repeated measures ANOVA $F_{(1.42)}$=0.00053, p=0.98 , Fig. 18A).

Although AM fibres in SLP3$^{-/-}$ mice had slightly increased mechanical latencies and individual mechanical latencies vary more strongly in SLP3$^{-/-}$ mice than in littermate controls, these results reflect no statistically significant differences between the genotypes (Fig. 18B). The median von Frey threshold in SLP3$^{-/-}$ mice (6.3mN) was significantly higher compared to SLP3$^{+/+}$ mice that exhibit a median von Frey threshold of 2.0mN (Mann-Whitney U test p=0.0078, data not shown). Thus, although the coding ability of a mechanical stimulus is not affected in AM fibres from SLP3$^{-/-}$ mice, these data suggest that the mechanical activation threshold of AM fibres is altered in SLP3$^{-/-}$ mice.

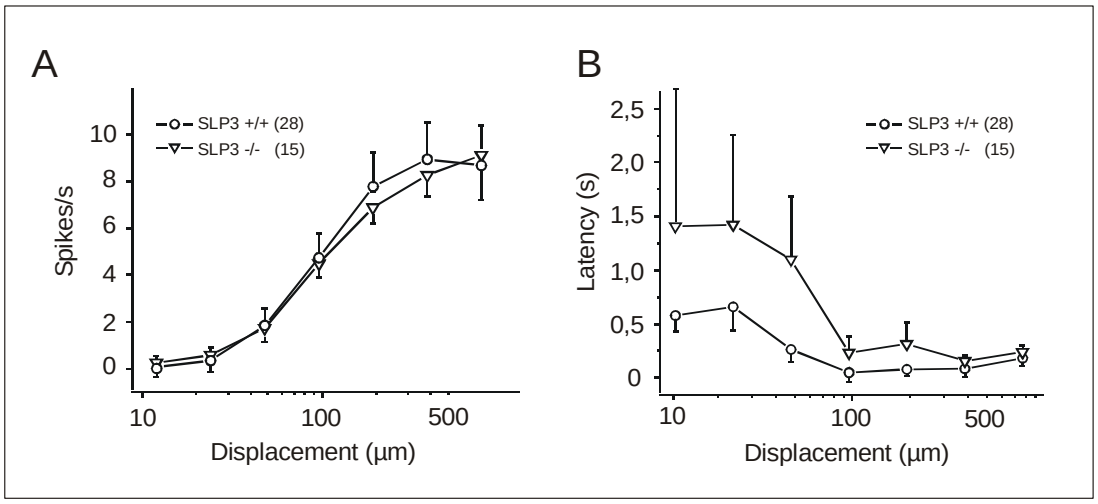

Figure 18 Mechanosensitivity of AM fibres in SLP3$^{-/-}$ mice
A) Mechanical properties of AM fibres concerning displacement stimulus response function were not different in SLP3$^{-/-}$ mice compared to wild-type littermates. **B)** Note that AM fibres in SLP3$^{-/-}$ mice exhibited longer mechanical latencies than in SLP3$^{+/+}$ mice, but this effect did not reach statistical significance (repeated measures ANOVA >0.05). Error bars indicate s.e.m.

3.3.4.5 Mechanosensitivity of C-fibres in SLP3$^{-/-}$ mice

C-fibres make up the largest category of cutaneous mechanoreceptors in mice (60%) (Koltzenburg et al., 1997). They can roughly be divided into C-mechanoheat receptors (C-MH) and C-mechanonociceptors (C-M). C-fibres forming exclusively free nerve endings in the skin have non-myelinated axons and subsequently conduct very slowly (<1.0m/sec in mice).

Twenty-five (SLP3$^{-/-}$) and 29 (SLP3$^{+/+}$) C-fibres were tested to produce a stimulus response function. Mechanical latencies were also determined. The firing frequency of the whole C-fibre population is similar between the genotypes (Fig. 19A). The mean mechanical latencies in C-fibres from SLP3$^{-/-}$ mice were slightly shorter, indicating that C-fibres in the mutants might have lower mechanical activation thresholds for eliciting action potentials following mechanical stimulation. However, this effect was not statistically significantly shorter in SLP3$^{-/-}$ mice compared to wild-type littermates (repeated measures ANOVA $F_{(6.36)}$ =0.65 p=0.688, Fig. 16B).

From 19 (SLP3$^{-/-}$) or 27 (SLP3$^{+/+}$) C-fibres, which were tested for heat sensitivity, 13 (SLP3$^{-/-}$) or 17 (SLP3$^{+/+}$) responded to heat stimulation, i.e. receptor proportion is similar between the genotypes (Chi-square test p=0.7, Fig.19D). Analysing stimulus

response function for both subclasses separately, no changes in displacement stimulus response function were observed for C-MH fibres indicating that the mechanosensitivity is not altered in this subclass by disruption of *slp3* (Fig. 19C). At higher displacement strengths (from 307µm to 614µm) the firing frequency to increasing displacement stimuli is reduced in C-M fibres from SLP3$^{-/-}$ mice up to approximately 20% compared to SLP3$^{+/+}$mice indicating that this C-fibre subclass might detect mechanical stimulation less appropriate compared to wild-type littermates. However, these differences did not reach statistical significance (unpaired T-test p=0.28 (307µm); p=0.056 (614µm), Fig. 19C).

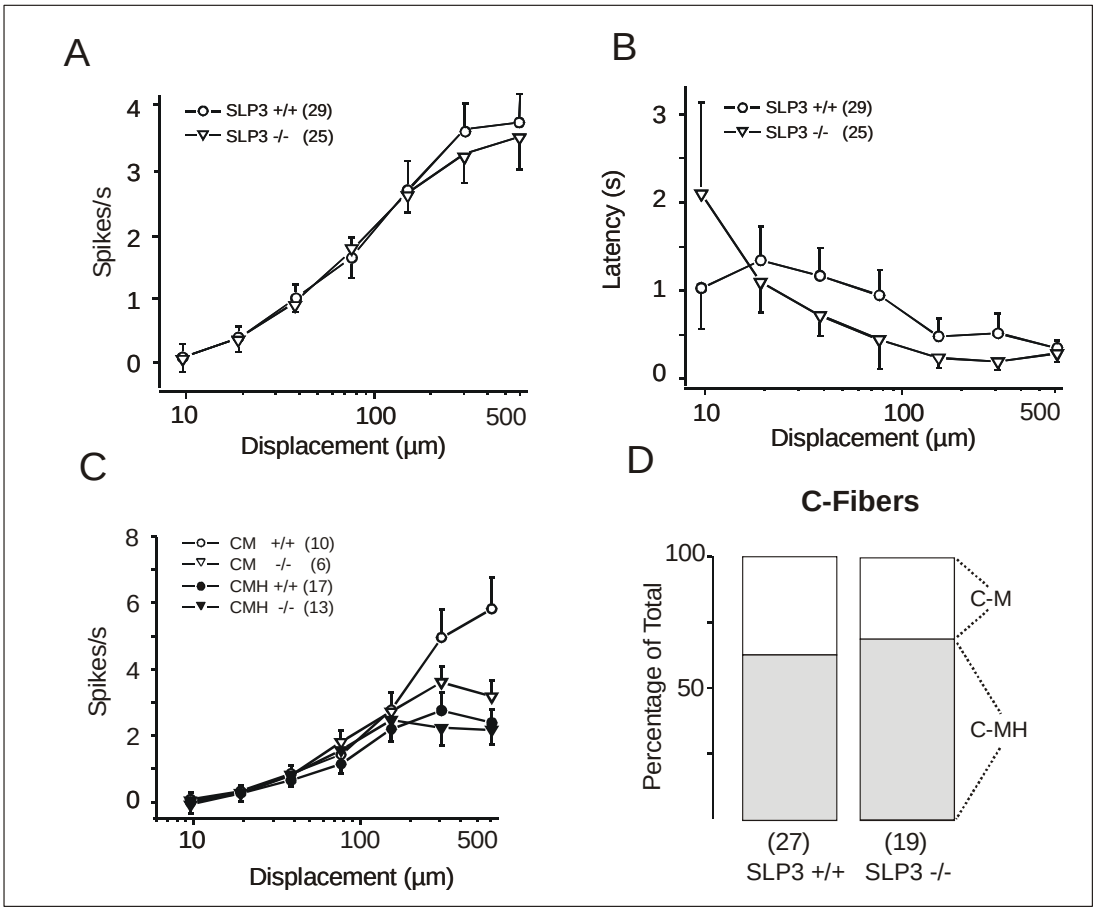

Figure 19 Mechanosensitivity of nociceptors in SLP3$^{-/-}$ mice
A) Displacement stimulus response function for the whole C-fibre population is shown. C-fibres from both genotypes exhibited similar mechanoreceptive properties. **B)** Mechanical latencies were slightly reduced in SLP3$^{-/-}$ compared to SLP3$^{+/+}$ mice without reaching statistical significance (repeated measures ANOVA p>0.05). **C)** Stimulus response functions of C-MH and C-M were analysed separately, but firing frequencies were not statistically significantly different between SLP3$^{-/-}$ and SLP3$^{+/+}$ mice (repeated measures ANOVA p>0.05 (C-MH) or T-test p>0.05 (C-M)). **D)** Receptor proportion is also unaffected in SLP3$^{-/-}$ mice compared to wild-type littermates (Chi-square test p>0.05). Error bars indicate s.e.m.

3.3.5 Lack of mechanoreceptor phenotype in SLP3$^{+/-}$ mice

Based on the fact that a transcript encoding the C-terminus of the *slp3* gene was amplified in RT-PCR using cDNA prepared from SLP3$^{-/-}$ mice it could be argued, that our mouse model does not represent a null mutation of the gene. The expressed *slp3* transcript might for example be translated into a SLP3 protein, which has a dominant negative effect. Dominant negative mutations often result in a gene product that adversely affects the wild-type protein. Subsequently, heterozygote mice carrying one mutant and one normal allele of the *slp3* gene should also develop mechanosensory insufficiencies. To test this possibility electrophysiological experiments were carried out, in which SLP3 heterozygotes (SLP3$^{+/-}$) were examined in the *in vitro* skin nerve preparation using the electrical search protocol.

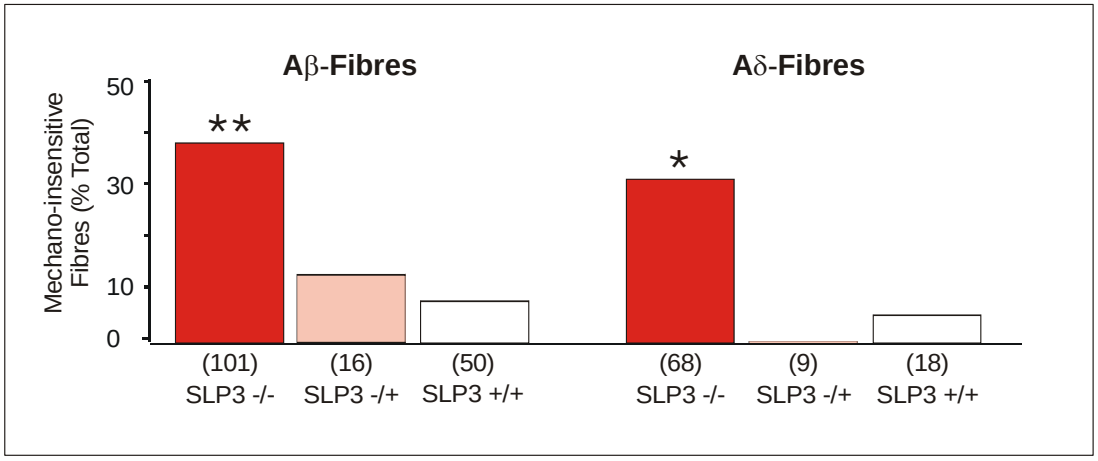

Figure 20 Mechanically insensitive sensory afferents in SLP3$^{+/-}$ mice
Thirty to forty percent of all A-fibre afferents in SLP3$^{-/-}$ mice lack mechanosensitivity compared to wild-type littermates (10%). Using an electrical search stimulus on SLP3$^{+/-}$ mice, in which the *slp3* locus is mutated in only one of the two alleles, the receptor proportion of mechano-insensitive fibres was similar to that found in control mice. (Chi-square test $p>0.05$ $^{**}p<0.005$). The numbers of single neurones recorded in each category are indicated below each column.

Twenty-five A-fibres isolated from three SLP3$^{+/-}$ mice were examined using electrical search stimuli. Nine units were classified as Aδ- fibres and 16 units as Aβ-fibres. All of the 9 Aδ-fibres tested had a mechanosensitive RF in the skin and produced normal stimulus response functions. Amongst the 16 Aβ-fibres tested, 2 units (12.5%) were classified as mechano-insensitve. This result shows that the proportion of mechano-insensitive fibres found in SLP3$^{+/-}$ mice is not different from

that found in wild-type littermates. Thus, most likely the mechano-insensitive phenotype we observed in SLP3$^{-/-}$ mice did not result from a dominant negative effect of any truncated SLP3 protein.

3.4 Mechanically gated ion channels require SLP3 for their function in mice

Since mechanoreceptor function abolished in at least 30-40% of A-fibres in SLP3$^{-/-}$ mice it seemed likely that SLP3 participates directly in the transduction mechanism. Mechanical forces applied on sensory neurones in culture also open mechanically gated ion channels directly and thus depolarise and excite the neurone. In collaboration with Dr. Jing Hu in our lab we asked whether SLP3 is required for the normal function of mechanosensitive ion channels expressed in acutely isolated sensory neurones from mouse DRGs.

Almost all sensory neurones from the DRGs cultivated on a laminin substrate produce mechanically gated currents (Fig. 21A and B). Depending upon their kinetic characteristics they can be classified as rapidly-adapting currents (RA) that activate and inactivate very quickly, intermediate-adapting currents (IA) with rapidly-adapting activation characteristics but slower inactivation kinetics or slowly-adapting currents (SA) (Hu and Sessle, 1988) (Hu and Lewin, 2006).

In wild-type mice >95% of isolated sensory neurones possess one of the mechanically gated currents described above: 52% (31/59 cells) RA, 29% (17/59 cells) SA, 15% (9/59 cells) IA. Three-point-four percent of the neurones tested in wild-type mice, i.e. only two of 59 cells did not possess any of these mechanically gated currents. This situation is completely different in SLP3$^{-/-}$ mice since thirty-six percent (21/58 cells) of the DRG neurones did not show any current response to mechanical stimulation of their neurites, an effect that was highly statistically significant (Chi-square test $p < 0.005$, Fig. 21C). This loss of mechanical excitability found in sensory neurones in SLP3$^{-/-}$ mice, appears to affect cells that have RA and SA currents similarly because the proportion of mechano-insensitive cells was reduced in both groups. This indicates that SLP3 might be required for both types of currents (Fig. 21C).

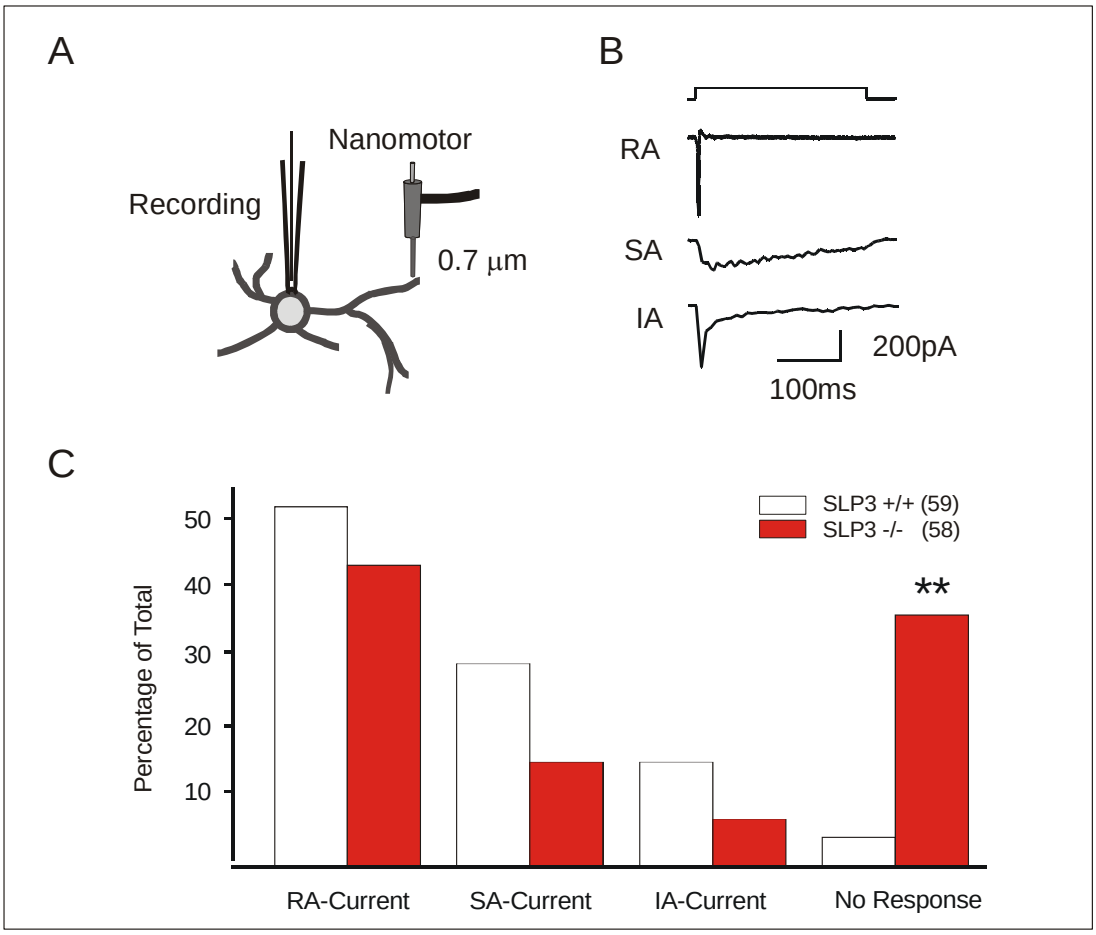

Figure 21 Mechanical activation of primary sensory neurones in SLP3$^{-/-}$ mice
A) Isolated DRG neurones were cultivated on poly-lysine and laminin. Newly formed neurites were stimulated mechanically using a miniature stepping motor (nanomotor). Whole cell responses were recorded from the cell soma under voltage clamp conditions in the presence of TTX. **B)** In control mice almost all neurones possess one of three types of membrane currents that can be classified as RA, SA or IA. **C)** The proportion of cells with one of the currents described above is plotted. Note that 36% of the neurones from SLP3$^{-/-}$ mice did not generate a mechanically gated current, and this is highly statistically significant (Chi-square test **p<0.005).

For direct involvement of SLP3 in the transduction of mechanical stimuli, it is hypothesised that the protein, like MEC-2 in *C. elegans,* interacts with a mechanosensitive transduction channel. Mutations of genes that encode ASIC proteins, which are members of the DEG/ENaC ion channel family, are proposed to participate in vertebrate mechanotransduction (Price et al., 2000), (Price et al., 2001). One of the ASIC family members, ASIC2, has shown to co-immunoprecipitate with SLP3 when transfected in a heterologous expression system (HEK293 cells). Expression of SLP3 in HEK293 cells results in a reduction of endogenously expressed proton-gated ion channels (Wetzel et al., Nature 2006 in press).

To address the question of whether the lack of the SLP3 protein could possibly lead to an incorrect targeting of one of the candidate ion channels, namely ASIC2, cultivated DRG neurones were obtained from 4 $SLP3^{-/-}$ mice for immunohistochemical analyses using a polyclonal antibody against ASIC2 (Price et al., 2000).
ASIC channels are found to be distributed in a highly punctuate manner in sensory neurones (Alvarez de la Rosa et al., 2002; Price et al., 2000).

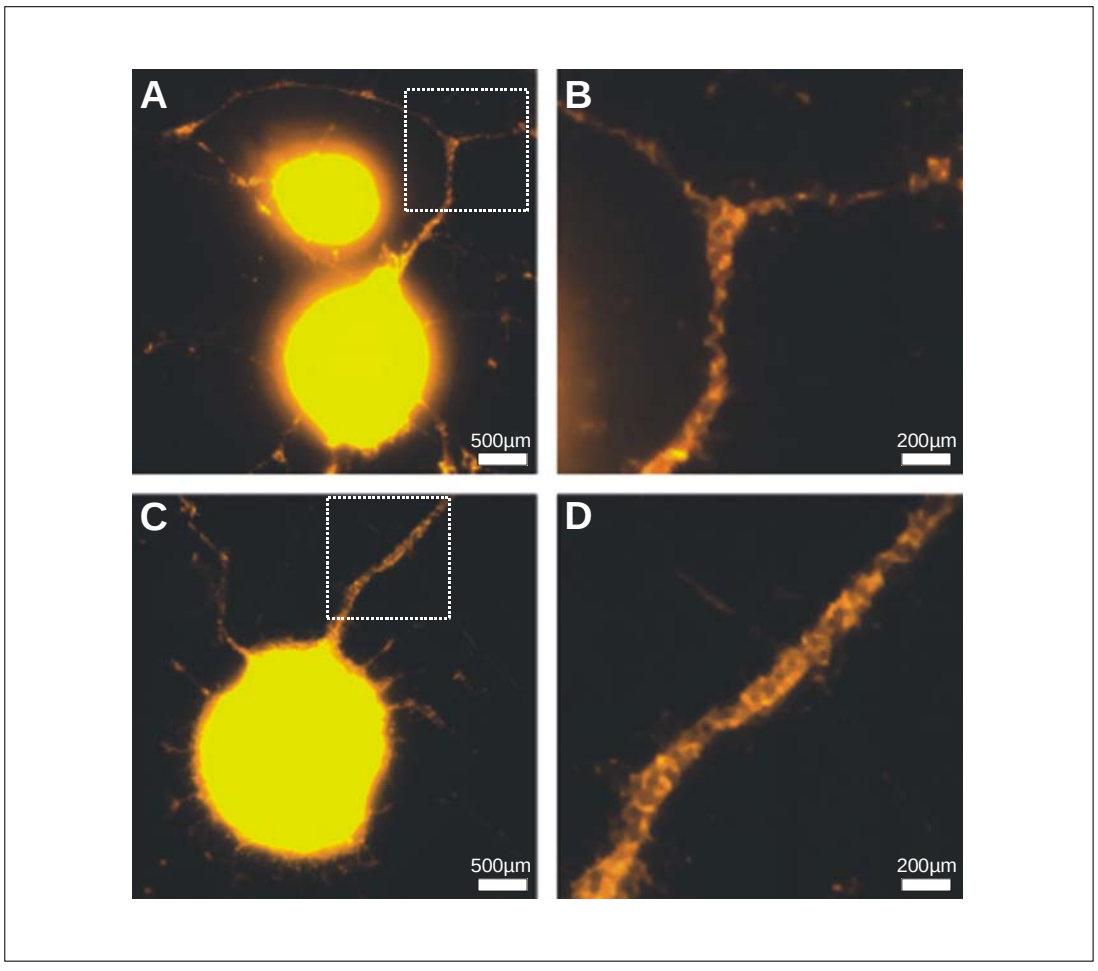

Figure 22 Expression of ASIC2 in $SLP3^{-/-}$ mice
Isolated DRG neurones obtained from $SLP3^{+/+}$ **(A** and **B)** and $SLP3^{-/-}$ mice **(C** and **D)** were cultivated on a poly-lysine and laminin substrate. Cells were stained for ASIC2 expression using a polyclonal antibody against an extracellular domain of the protein. Note that in $SLP3^{-/-}$ mice ASIC2 distribution in the membrane is still punctuated (lower panel) indicating that the absence of SLP3 does not cause mislocalisation of the ASIC2 ion channel.

In primary neurones obtained from $SLP3^{-/-}$ mice ASIC2 can clearly be localized to the membrane of the neurites and shows a punctuate distribution similar to that seen in wild-type littermates (Fig. 22 A and B). Thus, at least one candidate transduction

channel and member of the DEG/ENaC ion channel family is likely not mislocalised in the absence of SLP3.

3.5 Morphological integrity of sensory neurones and their afferent endings in the skin of SLP3$^{-/-}$ mice

The lack of SLP3 was found to affect mechanosensitivity in a broad range of myelinated primary afferents. Therefore we asked whether this effect could be explained by anatomical alteration of sensory axons in the peripheral nerve or their endings in the skin.

3.5.1 Sensory neurones in the saphenous nerve of SLP3$^{-/-}$ mice project normally to the skin

Saphenous nerves were obtained from 4 mice per genotype for electron microscopic analyses. Morphologically, axons of each size were indistinguishable in SLP3$^{-/-}$ mice compared to wild-type littermates. Non-myelinated C-fibre axons were grouped into structures called Remak bundles and myelinated neurones with medium and large size axons were uniformly distributed within the saphenous nerve (Fig.23A).
Two ultra thin sections were analysed per animal and genotype from which four digital images were taken representing an area of 333.4 µm^2. The total number of myelinated and non-myelinated axons was subsequently counted in the sampled area and extrapolated to the total area of the individual nerve (Fig.23B). In SLP3$^{-/-}$ mice approximately 2950 axons (673.9±117.02 myelinated A-fibres, and 2275.02±614.56 non-myelinated C-fibres) and in SLP3$^{+/+}$ animals approximately 2840 axons were counted (650.31±92.55 myelinated A-fibres and 2189.4±428.84 non-myelinated C-fibres). Thus, axon proportions found in SLP3$^{+/+}$ and SLP3$^{-/-}$ mice were identical resembling ~77% C-fibres and ~23% A-fibres. The mean diameter of myelinated axons in SLP3$^{-/-}$ mice was 3.26 ±1.23 µm and is therefore not statistically different compared to 3.5 ±1.26 µm in SLP3$^{+/+}$ mice (unpaired T-test p=0.056). The distribution of the axonal size quantified for A-fibre neurones in these nerves revealed no substantial differences between SLP3$^{-/-}$ mice and wild-type littermates

(Fig. 23C). Thus, there is no indication of any selective degeneration or death of sensory neurones in the saphenous nerve in SLP3$^{-/-}$ mice.

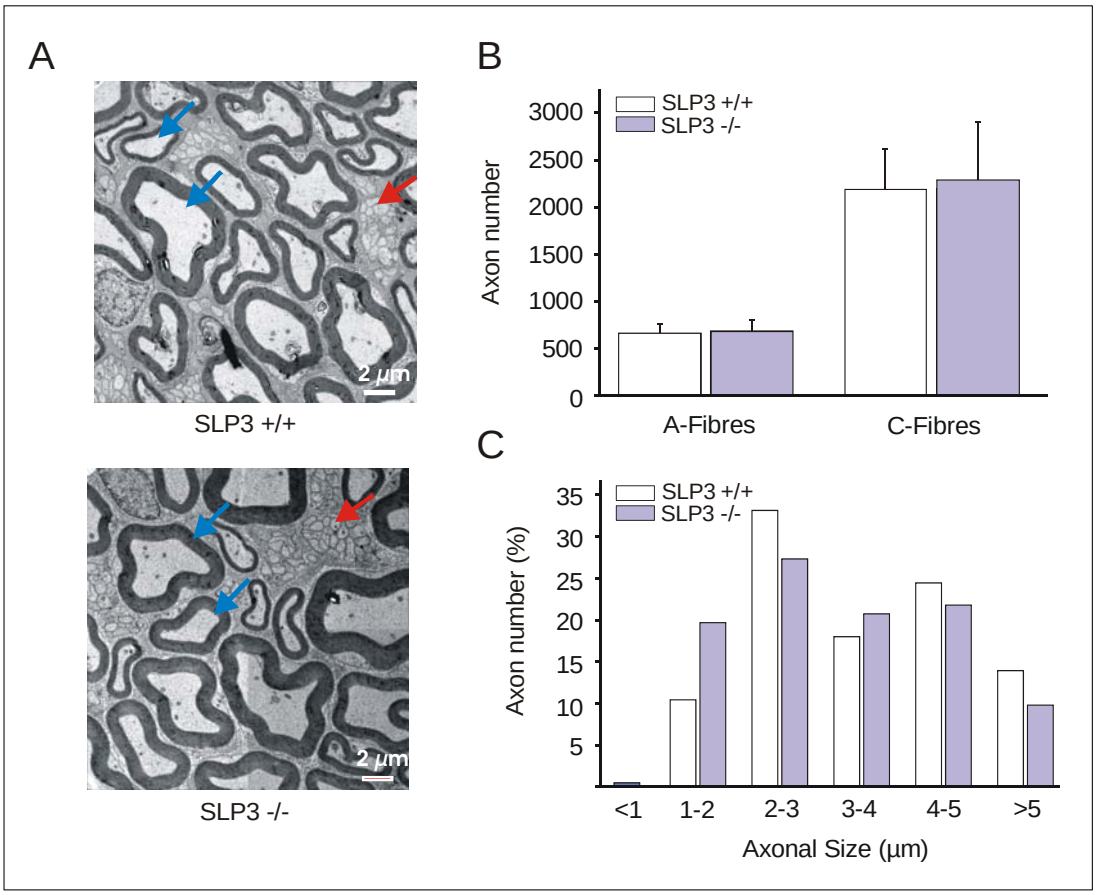

Figure 23 Electron microscopy of the saphenous nerve
A) Examples for a typical electron micrograph of the saphenous nerve (transverse section) of a SLP3$^{+/+}$ (upper panel) and SLP3$^{-/-}$ mouse (lower panel) are shown. Arrows indicate large diameter Aβ-fibres (blue) or small C-fibre axons within a Remak bundle (red). Scale bar is 2µm. **B)** Myelinated (A-fibres) and non-myelinated (C-fibres) axons were counted for a representative area of the nerve and extrapolated to the nerve cross-section to determine the total number of axons in each nerve. There was no difference in the total number of axons noted between the genotypes neither for A- nor for C-fibres (unpaired T-test $p>0.05$). **C)** The distribution of the axonal size of myelinated neurones in the saphenous nerve was also similar in both genotypes. Error bars indicate s.e.m.

Since a millisecond precision is functionally important for the nervous system and a conduction velocity of a neurone is determined by the diameter of the axon and its myelin sheath thickness, the integrity of the axon myelinisation in SLP3$^{-/-}$ mice was also measured. The thickness of myelin-forming Schwann cells that engulf the axonal segment of a fibre is proportional to the axonal diameter and the internodal length. This proportion is relatively constant between different species and nerves

(Friede, 1986; Friede and Bischhausen, 1982; Williams and Wendell-Smith, 1971). Thus, g-ratios reflecting the numerical ratio between the diameter of the actual axon and the outer diameter of the myelinated fibre were calculated from approximately 200 myelinated axons per genotype (n=4). The average g-ratio calculated from nerves obtained from $SLP3^{-/-}$mice was 0.72 ±0.05 and therefore not significantly different from $SLP3^{+/+}$ nerves (0.68 ±0.06). These results are consistent with conduction velocities measured in the skin nerve preparation (see Table 2) indicating that primary afferents in the saphenous nerve of $SLP3^{-/-}$ mice conduct normally.

3.5.2 Sensory afferents form morphologically normal endings in SLP $^{-/-}$ mice

Functional mechanosensitivity is a property of sensory endings in the skin. To test whether SLP3 is involved in dermal and/or epidermal sensory innervation, rather than in the transduction mechanism, skin sections were stained using immunohistochemical techniques. About 35 skin sections removed from the saphenous territory of 4 animals per genotype were labelled with a polyclonal antibody against the pan-neuronal marker ‘protein gene product 9.5’ (PGP9.5) (Reynolds and Fitzgerald, 1995) (Schofield et al., 1995). Skin sections were analysed blind whereas assessment criteria were specified separately for epidermal and dermal innervation differences. On an arbitrary scale the highest innervation density was quoted as 4 and the lowest innervation density as 1.

The sensory ending innervation density in the skin was analysed as a cumulative distribution function. The median values for the labelling intensity were 2.74 ($SLP3^{-/-}$) and 2.96 ($SLP3^{+/+}$) considering epidermal innervation density and 2.66 ($SLP3^{-/-}$) and 3.06 ($SLP3^{+/+}$) for dermal innervation of the skin (Mann-Whitney U-test p=0.77 (epidermis) p=0.155 (dermis), Fig. 24B). Thus, the dermis and epidermis seem to be similarly innervated by sensory afferents in both genotypes.

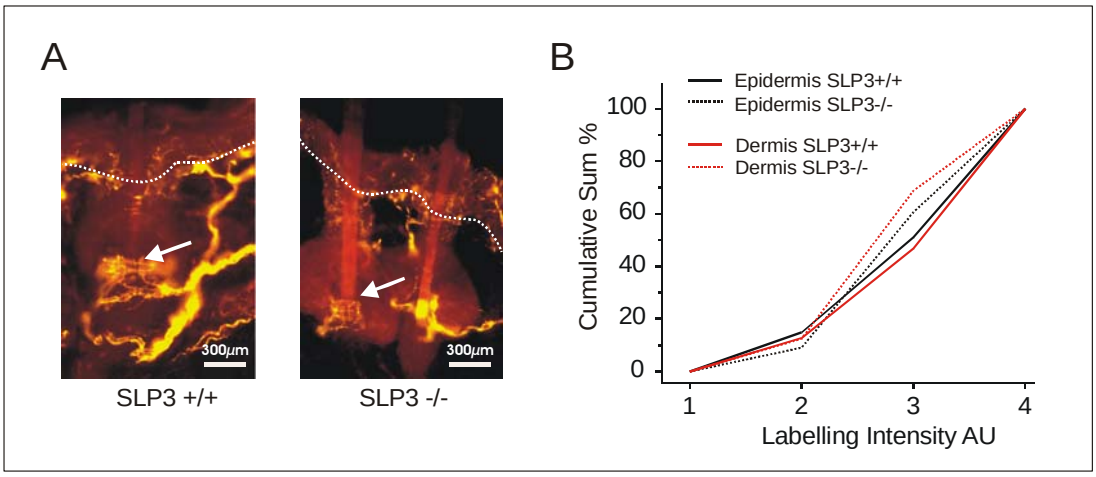

Figure 24 Sensory innervation of the hairy skin in SLP3$^{-/-}$ mice
A) Examples for a typical skin section stained with antibodies against the pan-neuronal marker protein PGP9.5. The dotted lines indicate epidermis-dermis boundaries. Arrows stress typical basket arrangements of sensory endings at the base of a hair follicle. Scale bars indicate 300µm. **B)** Quantitative analyses of the innervation density of the dermis and epidermis in SLP3$^{+/+}$ and SLP3$^{-/-}$ mice are shown. Approximately 35 skin sections per genotype were assessed blind on arbitrary scale. No statistically significant differences in the innervation density were observed between the genotypes (Mann-Whitney U-test $p>0.05$).

Besides of the complete loss of mechanosensitivity found in 30-40 % of all myelinated fibres, RAM fibres were most affected in SLP3$^{-/-}$ mice since ~45 % of RAM fibres did not respond to the fastest movement of the nanomotor. Hair movement (Petrini, 1999) usually stimulates rapidly-adapting mechanoreceptors, and in the saphenous nerve RAM fibres innervating hair follicle in mice are mostly lanceolate nerve endings or pilo-Ruffini endings. Whereas lanceolate endings surround the hair follicle by forming palisades running longitudinal to the hair shaft, pilo-Ruffini nerve endings form spirals around the lanceolate endings (Fig. 25A, schematic drawing).

In an additional experiment approximately 60 hair follicle of PGP9.5 stained skin section were examined for innervation with either lanceolate or pilo-Ruffini nerve endings. The endings were also counted under fluorescence illumination using 100 x oil immersion objective. The anatomical architecture of this innervation appeared normal in both genotypes (Fig. 25B). In SLP3$^{+/+}$ animals 39% and in SLP3$^{-/-}$ mice 48% of the hair follicles were surrounded by both lanceolate and pilo-Ruffini endings (Fig. 25C). Forty-five percent of the hair follicles in controls and 34% in SLP3$^{-/-}$ mice were innervated by one of the fibre types. Sixteen percent of the hair

follicle in SLP3$^{+/+}$ or nine percent in SLP3$^{-/-}$ did not show any PGP9.5 detectable innervation when observed with a 100 x oil immersion objective. The percentage of hair follicles that were innervated with either one or both types of receptor endings is therefore similar in both genotypes (Chi-square test p=0.56, Fig 25C). Hair follicles were on average surrounded by 6.38±2.35 palisades of lanceolate endings and/or by 3.69±1.71 pilo-Ruffini endings in SLP3$^{-/-}$ mice, but on average 6.31±2.02 lanceolate endings and/or 4.23±1.67 pilo-Ruffini endings were counted per hair follicle in SLP3$^{+/+}$ mice.

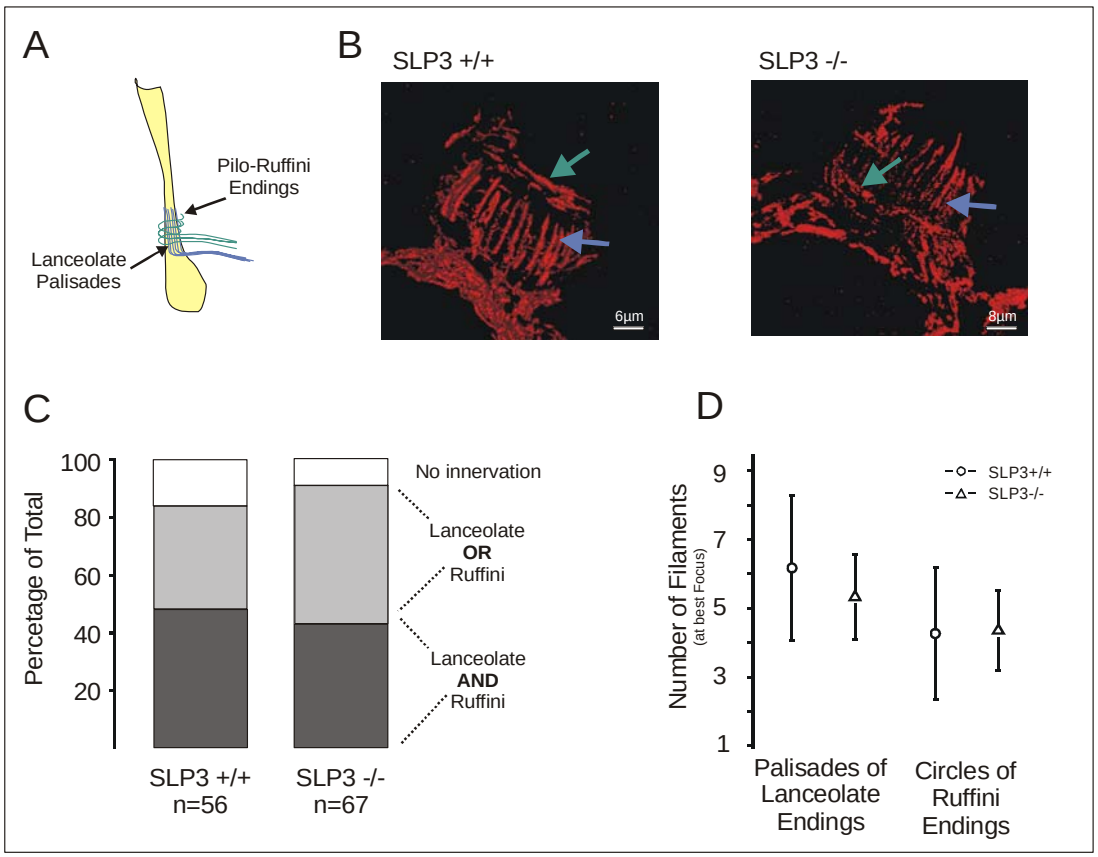

Figure 25 Hair follicle innervation in SLP3$^{-/-}$ mice
A) A schematic drawing of an innervated hair follicle is shown. **B)** Typical 3D views of an innervated hair follicle. Pictures, taken with a Zeiss LSM 510 microscope using 100 x oil immersion objective, show typical examples of lanceolate or pilo-Ruffini endings surrounding a hair follicle in a SLP3$^{+/+}$ (left) or a SLP3$^{-/-}$ mouse (right). Skin sections here were immunoassayed with anti-PGP9.5 antibody. Afferent endings are marked with either blue (lanceolate) or green (pilo-Ruffini) arrows. **C)** Approximately 50 hair follicles per genotype were analysed for sensory innervation with either lanceolate or pilo-Ruffini endings. Note that the same amounts, shown as percentage of total, of fibres were innervated with both types of sensory afferent endings as well as with only one fibre type in control and SLP3$^{-/-}$ mice (Chi-square test p>0.05). **D)** Palisades of lanceolate endings and circles of pilo-Ruffini endings were counted at best focal plane using 100 x oil immersion objective. No

statistically significant differences were observed between the genotypes (unpaired T-test $p>0.05$).

These data indicate that hair follicle innervation is similar in both genotypes (unpaired T-test $p=0.677$ (lanceolate) $p=0.35$ (Ruffini), Fig. 25D). Thus, neither qualitative nor quantitative changes in sensory endings in the skin could be found in $SLP3^{-/-}$ mice compared to wild-type littermates.

3.6 Investigation of SLP3$^{-/-}$/ Stomatin$^{-/-}$ mice

In mammals, including mice, the closest relative to SLP3 at the amino acid level showing 65% overall identity is stomatin. According to their amino acid sequence a hairpin like structure is predicted for both SLP3 and stomatin. Both proteins exhibit a short N-terminus and are anchored to the cell membrane via a membrane insertion domain that is followed by a long cytoplasm C-terminus. The latter has been shown to exhibit a putative protein interaction domain since both proteins were reliably pulled down in co-immunoprecipitation experiments when transfected into HEK 293 cells whereas C-terminal truncated constructs failed (Martinez-Salgado, Benckendorff, Wetzel & Lewin MS in prep). Stomatin is expressed by all sensory neurones of the DRG (Mannsfeldt et al., 1999). However, *stomatin* null mutant mice developed a relatively minor phenotype for cutaneous touch sensitivity. In electrophysiological experiments on sensory afferents in the skin, the only affected mechanoreceptors are low threshold D-hair receptors (Martinez-Salgado, Benckendorff, Wetzel & Lewin MS in prep). In order to validate whether the lack of both proteins would lead to more dramatic changes in touch sensation, we generated a double mutant mouse line lacking both *slp3* as well as *stomatin* gene products by interbreeding of the corresponding single mutants. Homozygote SLP3$^{-/-}$/Stomatin$^{-/-}$ mice are healthy, behave normally and lack any obvious pathology.

3.6.1.1 Mechanosensory properties in SLP3$^{-/-}$/ Stomatin$^{-/-}$ mice

In order to investigate mechanosensitive properties of low threshold and nociceptive mechanoreceptors in these mice the same *in vitro* skin nerve preparation protocols for electrical and mechanical search as carried out for SLP3$^{-/-}$ mice were used. Thirty-nine A-fibres and 14 C-fibres were investigated with the electrical search protocol (Table 3). Using the mechanical stimulation protocol extracellular recordings were made from 65 myelinated and 19 non-myelinated sensory afferents obtained from SLP3$^{-/-}$/Stomatin $^{-/-}$ and 98 myelinated and 35 non-myelinated fibres from wild type littermates (Table 4).

	SLP3$^{+/+}$/ Stomatin$^{+/+-}$ (electrical search)		SLP3 $^{-/-}$/ Stomatin$^{-/-}$ (electrical search)	
Receptor Type	**Number**	**% Total**	**Number**	**% Total**
Aβ-Fibres Aβ- units	50		22	
no RF	4	8.0	9	40.9
Aδ-Fibres Aδ- units	18		17	
no RF	1	5.6	6	35.3
C-Fibres C- units	20		13	
no RF	2	10.0	2	15.4

Table 3 Detailed breakdown of the single fibre recording in SLP3$^{-/-}$/Stomatin$^{-/-}$ and wild-type littermates using the electrical search protocol
Receptor proportion (% Total) of those mechanoreceptors that did not exhibit a mechanosensitive receptive field in the periphery is displayed as no RF.

	SLP3$^{+/+}$/ Stomatin$^{+/+}$ (mechanical search)			SLP3 $^{-/-}$/ Stomatin$^{-/-}$ (mechanical search)		
Receptor Type	**% Total**	**CV m/s**	**vFT**	**% Total**	**CV m/s**	**vFT**
Aβ-Fibres RAM	40.7 (22/54)	13.8±0.62	1.0 (0.4/6.3)	36.59 (15/41)	15.33±0.9	1.0 (0.4/1.0)
SAM	59.3 (32/54)	13.8±0.64	1.4 (0.4/13.0)	63.41 (26/41)	16.13±0.7	1.4 (0.4/10)
Aδ-Fibres AM	70.5 (31/44)	5.3±0.44	2.0 (1.0/13.0)	79.17 (19/24)	5.88±0.66	6.3 (1.0/22.0)
D-hair	29.5 (13/44)	4.5±0.51	0.4	20.83 (5/24)	5.1±0.32	0.4
C-Fibres C-units	(35)	0.53±0.03	10.0 (2.0-47.0)	(19)	0.56±0.07	6.3 (2.0-10.0)
C-M	37 (10/27)	0.62±0.07	6.3 (2.0-10.0)	38.46 (5/13)	0.65±0.17	6.3
C-MH	63 (17/27)	0.74±0.03	13.0 (3.3-22.0)	61.56 (8/13)	0.44±0.05	6.3 (2.0-6.3)

Table 4 Detailed breakdown of the single fibre recording in SLP3$^{-/-}$/Stomatin$^{-/-}$ and wild-type littermates using the mechanical search protocol
Receptor proportions (% Total), conduction velocities (CV) and mechanical thresholds (vFT, median values are shown with the 1st and 3rd quartile range) for individual mechanoreceptor classes. Means are expressed as ± s.e.m.

3.6.1.2 Mechano-insensitive fibres in SLP3$^{-/-}$/Stomatin$^{-/-}$ mice

Applying an electrical search stimulus to isolate single sensory afferents from SLP3$^{-/-}$/Stomatin$^{-/-}$ mice, 41% (9 of 22) of the Aβ-fibres and 35% (6 of 17) of the Aδ-fibres tested did not exhibit a mechanosensitive RF in the skin. Proportions of mechano-insensitive fibres in SLP3$^{-/-}$/Stomatin$^{-/-}$ mice were statistically significantly different from mechano-insensitive fibres found in wild-type littermates (Chi-square test $p<0.001$ (Aβ), $p=0.028$ (Aδ), Fig.23A) but proportional changes were not different from mechano-insensitive fibres found in SLP3$^{-/-}$ mice (Chi-square test $p=0.08$ (Aβ), $p=0.8$ (Aδ)). C-fibres that did not exhibit a RF were also found in SLP3$^{-/-}$/Stomatin$^{-/-}$ mice (15% (2 of 13 units)), but the proportional distribution was not different from wild-type littermates (Chi-square test $p=0.06$, Fig. 26A) or SLP3$^{-/-}$ mice (Chi-square test $p=0.69$). These data indicate that there is no additional effect concerning the number of the mechano-insensitive fibres in mice with an additional *stomatin* gene deletion, since approximately the same proportions of mechanically insensitive Aβ- and Aδ-fibres were also found in SLP3$^{-/-}$ mice.

As in our previous studies of SLP3$^{-/-}$ mice, the relative receptor proportion of the different mechanoreceptor subclasses, i.e. the ratio of RAM to SAM in Aβ-fibres, the ratio of AM to D-hairs in Aδ-fibres and C-M-fibres to C-MH-fibres were also not changed in SLP3$^{-/-}$/Stomatin$^{-/-}$ mice compared to wild-type littermates. In SLP3$^{-/-}$/Stomatin$^{-/-}$ mice 63.4% (26 of 41) of the Aβ-fibres were classified as SAM fibres and 39.6% (15 of 41) as RAM fibres. Amongst the Aδ-fibres 79.2% (19 of 24) were classified as AM and 20.8% (5 of 24) as D-hairs. Thirty-eight percent (5 of 13) of the C-fibres were classified as C-M-fibres and 61.5% (8 of 13) as C-MH-fibres (Fig. 26B). Thus, compared to wild-type littermates, as well as to SLP3$^{-/-}$ mice, there is no change in receptor distribution observed in SLP3$^{-/-}$/Stomatin$^{-/-}$ mice indicating that none of the receptor types seem to be selectively affected by deleting both genes.

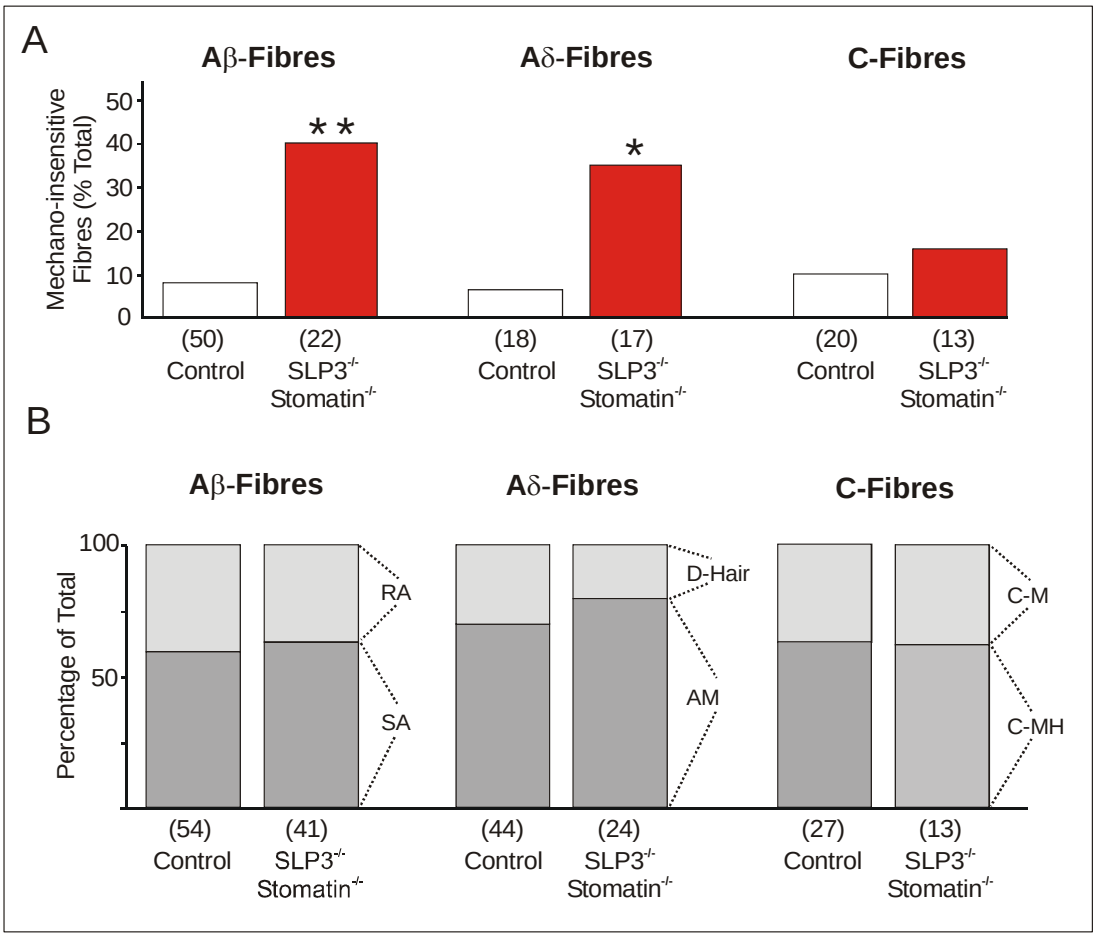

Figure 26 Mechanically insensitive sensory afferents in SLP3$^{-/-}$/Stomatin$^{-/-}$ mice
A) The electrical and mechanical search protocols were used. In SLP3$^{-/-}$/Stomatin$^{-/-}$ mice a statistically significant different proportion of mechano-insensitive afferents was found for A-fibres (Chi-square test **p<0.005 *p<0.05) but not for C-fibres (Chi-square test p>0.05) when compared to wild-type littermates. Numbers of fibres recorded in each category are indicated below each column. **B)** The proportion of mechanosensitive fibres, i.e. the ratio of RAM to SAM fibres amongst the Aβ-fibres and AM to D-hairs in the Aδ-range as well as the ratio of C-M to C-MH fibres was not changed in SLP3$^{-/-}$/Stomatin$^{-/-}$ mice (Chi-square test p>0.05) compared to controls. Numbers of single fibres recorded in each category are indicated below each column.

3.6.1.3 Mechanosensitivity of low threshold mechanoreceptors in SLP3$^{-/-}$/Stomatin$^{-/-}$ mice

Using the same mechanical stimulation protocol as previously used for SLP3 single mutants, the coding ability of low threshold mechanoreceptors was systematically examined. A range of quantitative mechanical stimuli was applied to the skin in order to investigate the sensitivity of mechanoreceptors to displacement as well as velocity stimulation in SLP3$^{-/-}$/Stomatin$^{-/-}$ mice. In the absence of both proteins

mechanosensitive properties of D-hair receptors were altered in SLP3$^{-/-}$/Stomatin$^{-/-}$ mice. Five D-hairs from SLP3$^{-/-}$/Stomatin$^{-/-}$ mice and 11 D-hairs from wild-type littermates were studied and the firing frequency to a series of increasing displacement stimuli was analysed for the dynamic movement response. The stimulus response function was largely reduced by about half in SLP3$^{-/-}$/Stomatin$^{-/-}$ mice compared to wild-type littermates and this effect reached statistical significance at 192µm displacement (unpaired T-test p=0.0036, Fig.27A). Except for the lowest velocity, to which only one of 5 fibres responded, the velocity response function shows a slight, but clear, rightward shift in SLP3$^{-/-}$Stomatin$^{-/-}$ mice when compared to wild-type littermates. The firing frequency of D-hairs at 0.7µm/msec is significantly lower in SLP3$^{-/-}$/Stomatin$^{-/-}$ mice compared to wild-type littermates (T-test p=0.045).

The coding ability of sensory afferents classified as SAM fibres was also studied. Here 21 fibres obtained from SLP3$^{-/-}$/Stomatin$^{-/-}$ mice and 24 fibres from wild-type littermates were investigated, but the absence of both proteins did not cause any sensitivity changes in SAM fibres compared to wild-type littermates (repeated measures ANOVA $F_{(6, 228)}$=0.214, p=0.972, Fig.27C).

Similar to SLP3$^{-/-}$ mice, a certain proportion of RAM fibres were classified as “tap” units. With 27% (4 of 15) “tap” units amongst all RAM fibres isolated from SLP3$^{-/-}$/Stomatin$^{-/-}$ mice the proportion is not statistically significantly different compared to 45% (9 of 20) “tap” units observed in SLP3$^{-/-}$ mice (Chi-square test p=0.76). As shown in figure 27D the remaining “non-tap” RAM fibres (11 units from SLP3$^{-/-}$/Stomatin$^{-/-}$ mice, 20 units from wild-type littermates) produced a stimulus response function to velocity stimulation with firing frequencies exhibiting similar properties in both genotypes (repeated measures ANOVA $F_{(6, 6)}$ =0.136, p=0.98, Fig. 27D).

In addition, other parameters investigated for low threshold mechanoreceptors in SLP3$^{-/-}$Stomatin$^{-/-}$ mice, such as mechanical latency (RAM, SAM, D-hair), stimulus response to the dynamic phase of displacement stimulations (SAM, RAM) or stimulus response to velocity stimulations (SAM), were not different from those observed in wild-type littermates (data not shown).

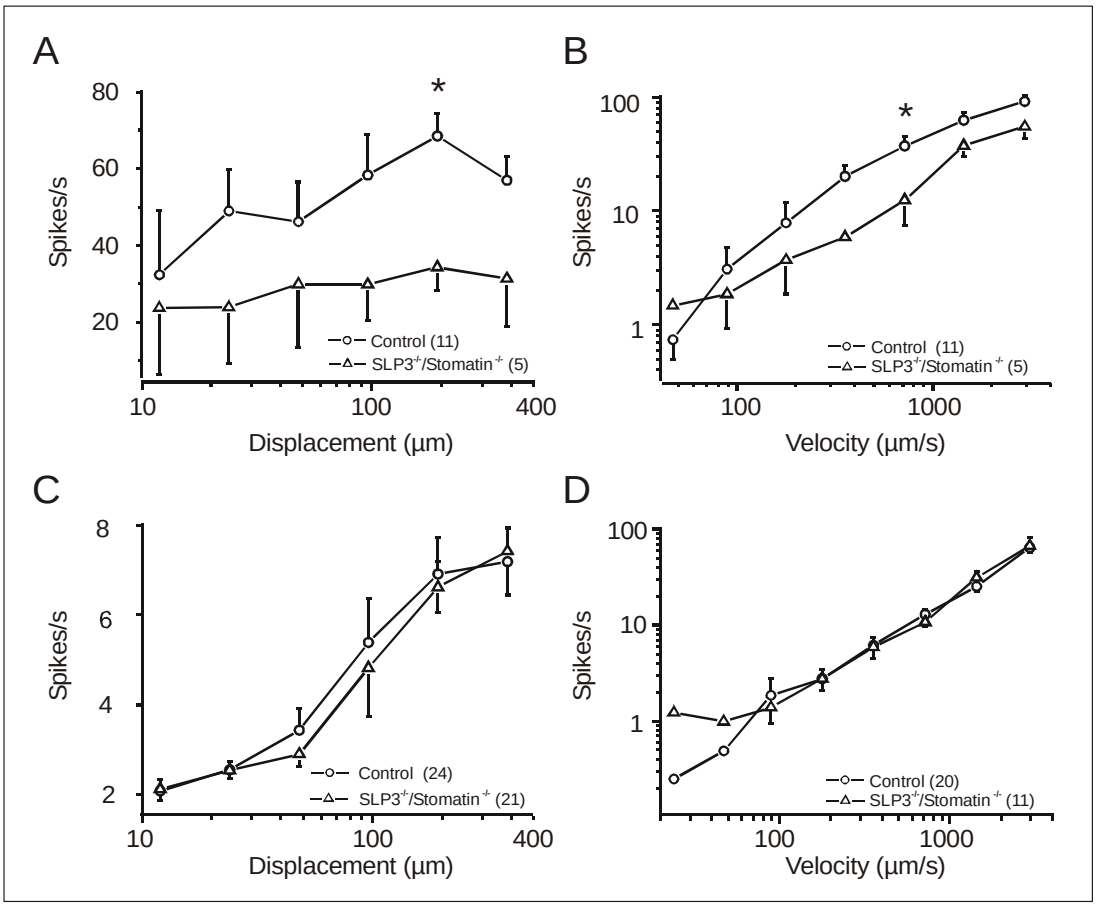

Figure 27 Mechanosensitivity of LTM fibres in SLP3$^{-/-}$/Stomatin$^{-/-}$ mice
Displacement and velocity stimulation protocols were used. Action potentials generated during the whole or only the dynamic phase of the stimulus were summed and the firing frequency per second was calculated. **A, B)** In SLP3$^{-/-}$/Stomatin$^{-/-}$ mice D-hair mechanoreceptors responded to displacement as well as velocity stimulation with firing less action potentials than D-hairs in wild-type littermates and this was significant where indicated (unpaired T-test *p<0.05) **C)** SAM fibres were not affected in SLP3$^{-/-}$/Stomatin$^{-/-}$ mice compared to wild-type littermates (repeated measures ANOVA p>0.05). The stimulus response function for the whole 10-second stimulus per indentation is plotted (. **D)** Velocity response function for RAM fibres revealed no changes in firing frequencies in SLP3$^{-/-}$ /Stomatin$^{-/-}$ mice compared to wild-type littermates (repeated measures ANOVA p>0.05). All error bars are indicated as s.e.m.

3.6.1.4 Mechanosensitivity of nociceptive receptors in SLP3$^{-/-}$/Stomatin $^{-/-}$ mice

Stimulus response functions were recorded for application of an ascending series of indentation stimuli to 19 (SLP3$^{-/-}$/Stomatin$^{-/-}$) or 28 (wild-type littermates) AM fibres. In contrast to SLP3$^{-/-}$ mice, AM fibres in SLP3$^{-/-}$/Stomatin$^{-/-}$ mice responded to mechanical displacement stimulation with firing slightly fewer action potentials at indentation strengths above 96 µm, but this did not reach statistical significance compared to wild-type littermates (repeated measures ANOVA $F_{(3.129)}$=0.52 p=0.67,

Fig. 25A). Similar to SLP3$^{-/-}$ mice, mechanical activation thresholds were found to be higher compared to wild-type littermates (Fig. 28B).

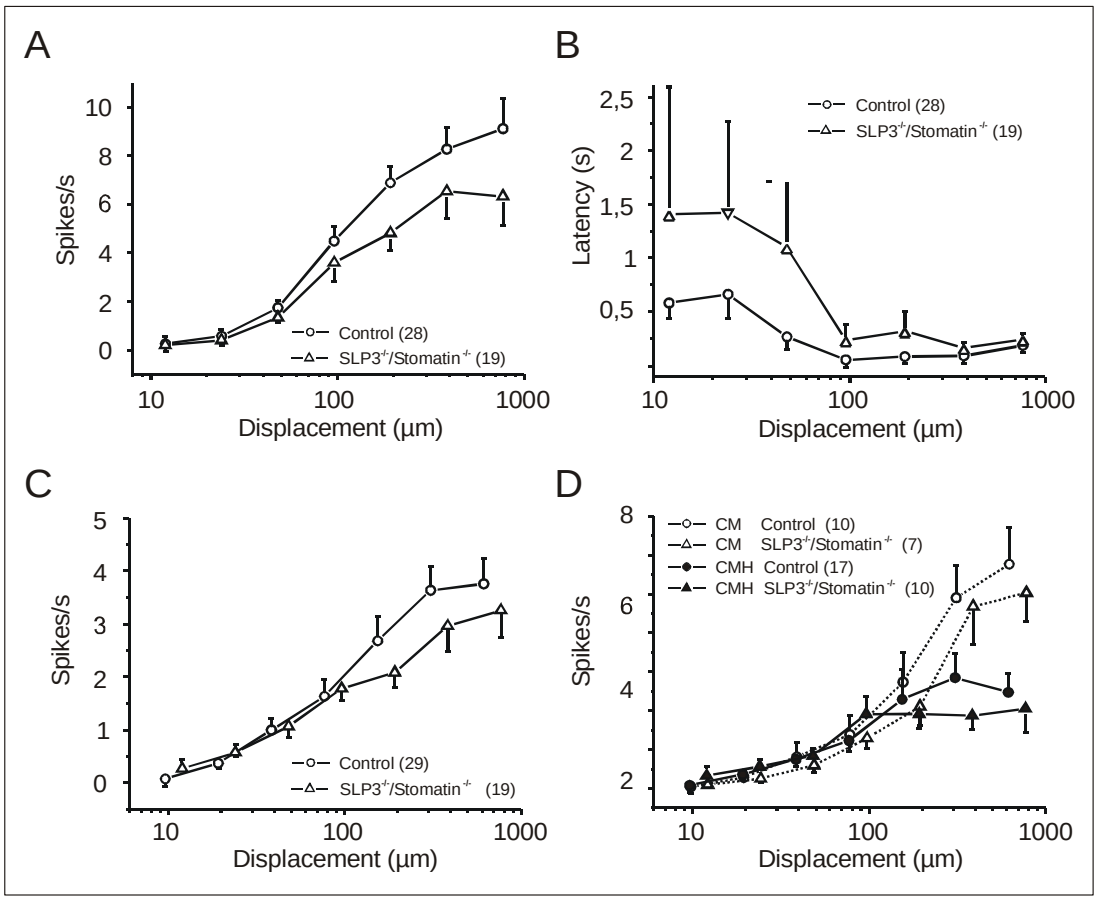

Figure 28 Mechanosensitivity of nociceptors in SLP3$^{-/-}$/Stomatin$^{-/-}$ mice.
An ascending series of indentation stimuli was applied to sensory afferents in the skin. Responses, i.e. action potentials fired during the 10-second displacement stimulations were averaged for each stimulus strength and displayed as action potentials per second. Mechanical latencies are shown only for AM fibres. **A, B)** AM fibres showed a reduced stimulus response function at higher displacement strengths (left) and compared to wild-type littermates. Mechanical latencies were on average increased at the first three stimulation strengths (right) in SLP3$^{-/-}$/Stomatin$^{-/-}$ mice. **C, D)** C-fibres showed a slightly impaired mechanical sensitivity (left) that could neither be addressed to C-M nor to C-MH fibres. However, all effects seen in SLP3$^{-/-}$/Stomatin$^{-/-}$ mice did not reach statistical significance (repeated measures ANOVA $p>0.05$). Error bars indicate s.e.m.

However, this effect was also not significantly different compared to mechanical latencies recorded from AM fibres in wild-type littermates (repeated measures ANOVA $F_{(5.9)}=0.52$ $p=0.76$, Fig. 28B).

Recordings from C-fibre nociceptive afferents isolated from SLP3$^{-/-}$/Stomatin$^{-/-}$ mice also did not reveal statistically significant differences in their stimulus response characteristics compared to wild-type littermates. However, at higher displacements (from 192-786µm) a slight rightward shift of the curve was observed in SLP3$^{-/-}$

/Stomatin$^{-/-}$ mice indicating that mechanosensitivity might be reduced in C-fibres from the double mutants, an effect that was not statistically significant (repeated measures ANOVA $F_{(2.86)}$=0.00472 p=0.98, Fig. 28C). This effect could be caused by changes in both C-M as well as C-MH receptors. A slight rightward shift of the stimulus response curve was observed for both nociceptor subclasses, but for neither C-M nor C-MH fibres it reached statistical significance compared to C-M or C-MH fibres obtained from control mice (repeated measures ANOVA $F_{(6.\ 78)}$ =0.14 p=0.99 (C-M fibres), $F_{(6.\ 114)}$ =1.0630, p=0.38897 (C-MH fibres), Fig. 28D).

3.6.2 Sensory neurones and sensory afferents are intact in SLP3$^{-/-}$/Stomatin$^{-/-}$ mice

To check that the anatomical integrity of sensory neurones was also not affected in SLP3$^{-/-}$/Stomatin$^{-/-}$ mice the same types of experiments as for SLP3$^{-/-}$ mice were performed. Saphenous nerves were removed from four animals per genotype and prepared for electron microscopy. Axon numbers of myelinated and non-myelinated neurones present in the nerve were then counted as described earlier. In SLP3$^{-/-}$ /Stomatin$^{-/-}$ mice approximately 3292 axons (664.96±142.88 myelinated A-fibres, and 2631.76±587.01 non-myelinated C-fibres) and in controls approximately 2750 axons were counted (650.31±92.55 myelinated A-fibres, and 2189.4±428.84 non-myelinated C-fibres). Results revealed no significant differences in total axon number for A- as well as for C-fibres (unpaired T-test p=0.81 (A-fibres), p=0.192 (C-fibres), Fig 29B). Thus, these results indicate that sensory neurones do not undergo neurodegeneration due to the lack of both SLP3 and stomatin.

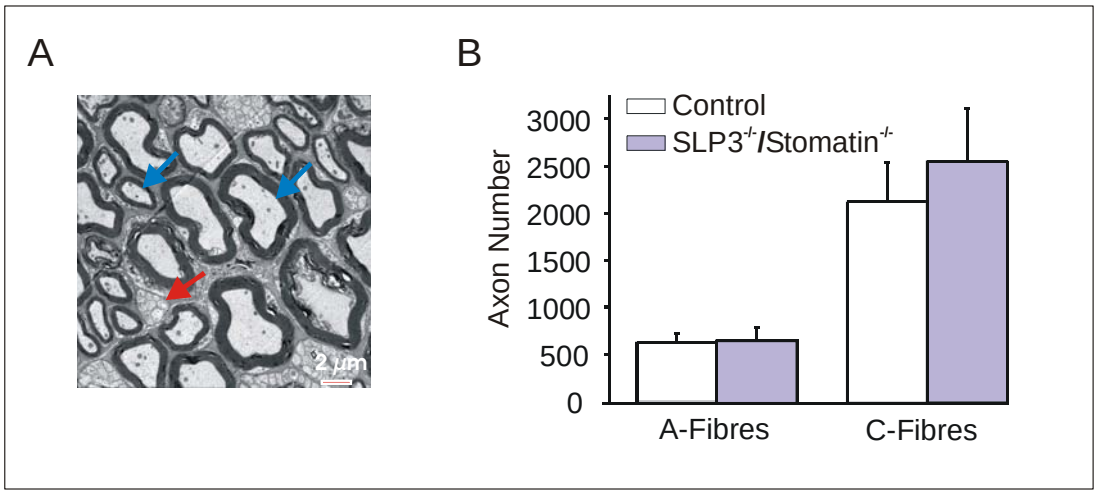

Figure 29 Electron microscopy of the saphenous nerve of SLP3$^{-/-}$/Stomatin$^{-/-}$ mice
A) An electro micrograph of a transverse section from the saphenous nerve is shown for SLP3$^{-/-}$/Stomatin$^{-/-}$ mice. Arrows indicate large and medium size A-fibre axons (blue) or non-myelinated C-fibre axons within a Remak bundle (red). Scale bar is 2µm. All axons of a representing area were counted and extrapolated to the nerve diameter. **B)** There was no difference in the total number of axons noted between the genotypes neither for A- nor for C-fibres. Error bars indicate s.e.m.

In order to examine dermal and epidermal mechanoreceptor innervation, skin sections of the saphenous nerve innervation territory were stained with antibodies against PGP9.5 (Reynolds and Fitzgerald, 1995) (Schofield et al., 1995) as described earlier for SLP3$^{-/-}$ mice. Results indicate that the innervation density of the skin by afferent endings is lower in the skin of SLP3$^{-/-}$/Stomatin$^{-/-}$ mice compared to controls, and this effect is statistically significant in the case of both epidermal (Mann-Whitney U-test p=0.049) and dermal innervation density (Mann-Whitney U-test p=0.003, Fig. 30B).

Interestingly, hair follicles, which are mostly innervated by RAM fibres, did not show any obvious morphological changes in the innervation pattern compared to that observed in wild-type littermates. In wild-type animals 39% but in SLP3$^{-/-}$/Stomatin$^{-/-}$ mice 44% of the hair follicles were surrounded by both lanceolate and pilo-Ruffini endings. Forty-five percent of the hair follicles in both wild-type littermates and SLP3$^{-/-}$/Stomatin$^{-/-}$ mice were innervated by one of the fibre types. Only 16% (wild-type littermates) and 12% (SLP3$^{-/-}$/Stomatin$^{-/-}$) did not show any PGP9.5 detectable innervation using 100 x microscopic magnification (Fig. 30C). No changes in the number of lanceolate palisades or pilo-Ruffini circles counted at the best focal plane could be observed in SLP3$^{-/-}$/Stomatin$^{-/-}$ mice (5.85±1.9 lanceolate endings; 4.56±1.76 pilo-Ruffini endings) compared to wild-type littermates (6.18±2.11

lanceolate endings; 4.27±1.93 pilo-Ruffini endings) (unpaired T-test p=0.94 (lanceolate) p=0.066 (Ruffini), Fig 30D). Thus, these data demonstrate that myelinated and non-myelinated sensory afferents in the skin appear to form normal endings in SLP3$^{-/-}$/Stomatin$^{-/-}$ mice compared to wild-type littermates.

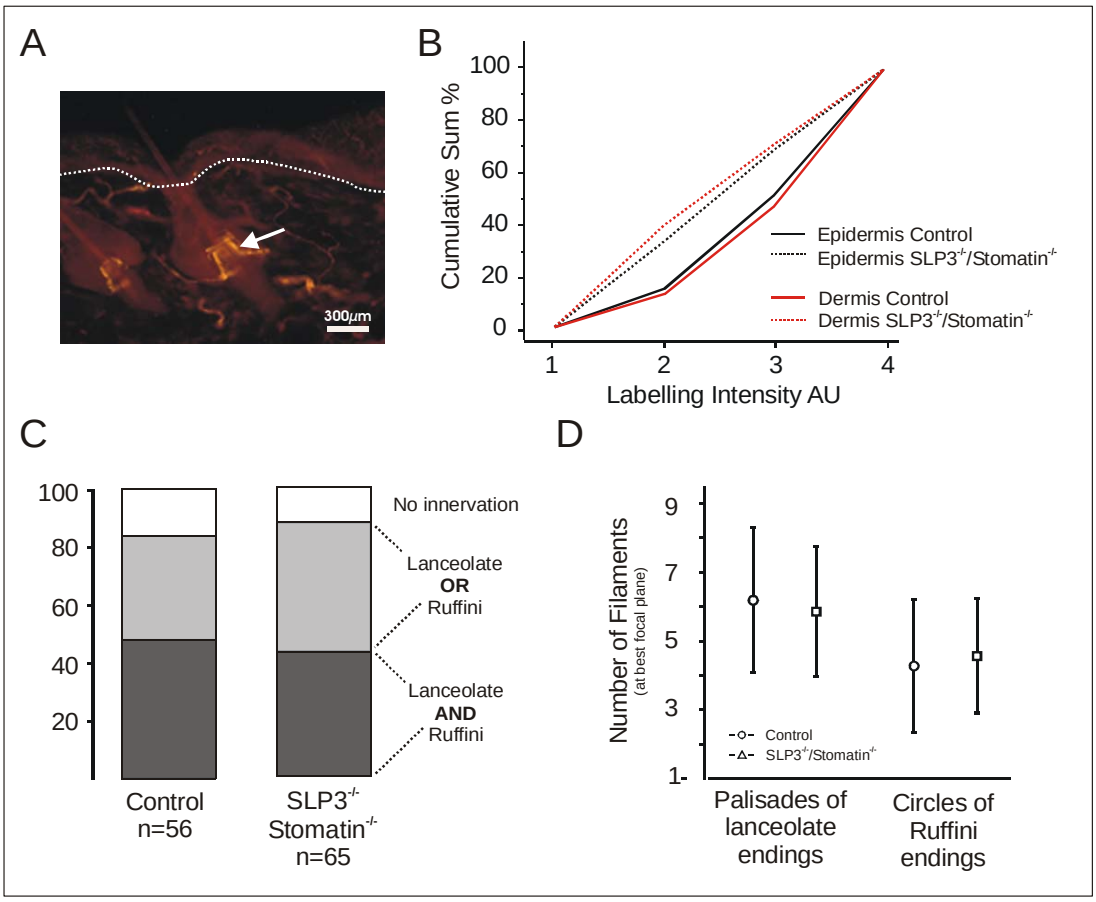

Figure 30 Sensory innervation of the hairy skin in SLP3$^{-/-}$/Stomatin$^{-/-}$ mice
A) Example of a typical skin section obtained from SLP3$^{-/-}$Stomatin$^{-/-}$ mice stained with antibodies against PGP9.5. The dotted line indicates the epidermis-dermis boundary; the arrow indicates a typical basket arrangement of sensory endings at the base of the hair follicle. **B)** Quantitative analyses of the innervation density of the dermis and epidermis in wild-type littermates and SLP3$^{-/-}$/Stomatin$^{-/-}$ mice revealed significant differences (Mann-Whitney U-Test p<0.05). **C)** A quantitative analysis of about 50 hair follicles innervated with either lanceolate or pilo-Ruffini endings is shown. Note that the same proportion of fibres was innervated with both types of sensory fibres as well as with only one fibre type in SLP3$^{-/-}$/Stomatin$^{-/-}$ mice compared to wild-type littermates (Chi-square test p>0.05).
D) Filaments of lanceolate and Pilo-Ruffini endings were counted at the best focal plane, numbers were similar in both genotypes (unpaired T-test p>0.05). Error bars indicate s.e.m.

3.7 Tactile driven behaviour is impaired in SLP3$^{-/-}$ mice

The loss of mechanosensitivity found in 30-40 % of myelinated primary afferents in SLP3$^{-/-}$ mice suggests that these mice might perceive touch stimuli differently. Since no suitable behavioural tests were available for investigating tactile acuity in mice we decided to develop such a test. This test is based on the introduction of surface cues exhibiting tactile properties. These tactile cues were exposed to the mice in a controlled environment (a featureless plastic box in the dark).
The test was designed to address the question whether mice in general and SLP3$^{-/-}$ mice in particular are able to detect and subsequently discriminate surface cues from the surrounding area. This might be shown through behavioural responses such as interest, attraction or also possibly avoidance. Accordingly, surface cues made of sandpaper and later custom-made plastic grids were chosen.

3.7.1 Design of a novel tactile acuity test for mice

Using the ActiMot system (TSE Systems GmbH) this test is based on an activity measuring system for small laboratory animals such as rats and mice for studying the animals' open field activity. The ActiMot system consists of a square base frame arranged at right angles to each other with two pairs of light barrier strips, in which each pair contains a transmitter and a receiver strip. The light barriers are arranged in the same plane to assure the determination of the x- and y-coordinates and therefore the exact location (x-y-plane) of the animal during activity measurement. (In principle it is also possible to mount an additional strip pair in z-orientation to detect vertical activity.) The test animal, in our case a mouse, is kept in the inner box made of clear Plexiglas, which is inserted into the frame (Fig. 31A). Via a process control unit containing the electronics for recording the activity or movement of an animal, the light barrier frame is connected to a special interface in the computer. Using ActiMot software controlling the complete system, light sensors are scanned sequentially, so that the position of the animal can be assessed every 10 milliseconds.

MoTil frames that were used for this behavioural test have a size of 350 x 480mm and are equipped with 6 x 12 light sensors, 28mm apart. Since the body of a mouse usually covers more than one light barrier, coordinates of the “centre of gravity” of the animal are calculated by averaging blocked light barriers (Fig. 31B). Subsequently the number of the possible positions calculated as x-y-coordinates of the animal’s location is doubled compared to the actual density of the light barriers, i.e. the spatial resolution of the system is half the distance (in this case 14mm) of the inserted light sensors.

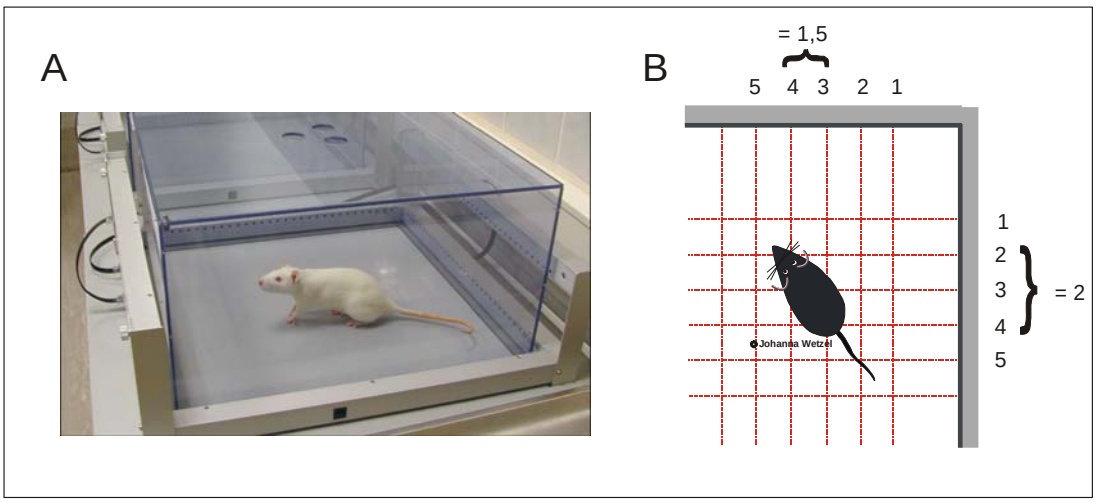

Figure 31 The TSE ActiMot system for measuring open field activity in mice
A) A square base frame arranged at right angles to each other consists of two pairs of light sensor strips. Light sensors are sequentially scanned every 10msec to determine x-y-coordinates and therefore the exact location of the mouse during activity measurement.
B) Since a mouse normally covers more than one light barrier, virtual x-y-coordinates are calculated as “centre of gravity“ by averaging blocked light barriers. Consequently, the spatial resolution is half the distance of two adjacent light sensors.

The ActiMot analysis software differentiates between two possibilities: “time resting” means that the animal persists at a certain position or moves only below activity threshold defined by the experimenter, “time moving” reflects the movement of the animal above the threshold.

In principle, an activity/locomotion and a spatial analysis can be performed on the data set in order to assess the motility of the animal in the vicinity of the tactile cue compared to a blank control insert, which exhibits the same tactile quality as the floor plate. The vicinity of the tactile cue or the control insert respectively was defined as the area quadrant. The activity/locomotion behaviour was analysed as

"distance travelled" and describes the walking behaviour of the mouse within the quadrants. The spatial resolution is calculated as "time visiting" reflecting the time the mouse spends in the vicinity of the cues (area quadrants). For analysis of spatial distribution, the box is virtually divided into 253 elements according to the given number of practical and virtual light barriers (11 x 23).

3.7.2 Behaviour of SLP3$^{-/-}$ mice on natural sandpaper

Initially wild-type C57BL/6N mice were examined using irregularly shaped compression-moulded plastic inserts with either coarse or fine structured properties serving as putative tactile surfaces. Neither of these surfaces turned out to be suitable for testing tactile acuity in mice since no measurable behavioural responses were detectable when C57BL/6N mice were tested on these cues (data not shown).

We went on to develop an improved test using tactile cues made of natural sandpaper, which have previously been used by Guic-Robles, who had shown that rats are able to discriminate sandpaper cues with the aid of their vibrissae (Guic-Robles et al., 1989).
Two tactile cues were placed flush to the surface of the cage floor plate, which was made of a slightly roughened Plexiglas in order to make it easier for the mice to walk around on the otherwise slippery ground (Fig. 32A and B). Since one of the surfaces was the rough (roughness grade =40) and the other the smooth (paper) side of the sandpaper (CRAFTOMAT, Bahag AG, Mannheim) both had the same olfactory quality. Data were collected from 12 adult mice (6 female, 6 male) per genotype. Since the SLP3$^{-/-}$ mouse line was at that time successfully backcrossed on C57BL/6N genetic background, we used the latter as control. Each mouse was tested twice, namely in the so-called positive experiment (Fig. 32B) in which sandpaper cues were exposed to the animal by placing them randomly into two of the four possible positions, but also in a negative experiment (Fig. 32A) where no tactile cues but blank control inserts were placed into the floor plate. The experiments were performed in complete darkness, thus mice could detect the new tactile surface only by using their sense of touch or smell. Normal background activity in the absence of any tactile cue was examined for 30 min prior to the exposure to novel tactile cues.

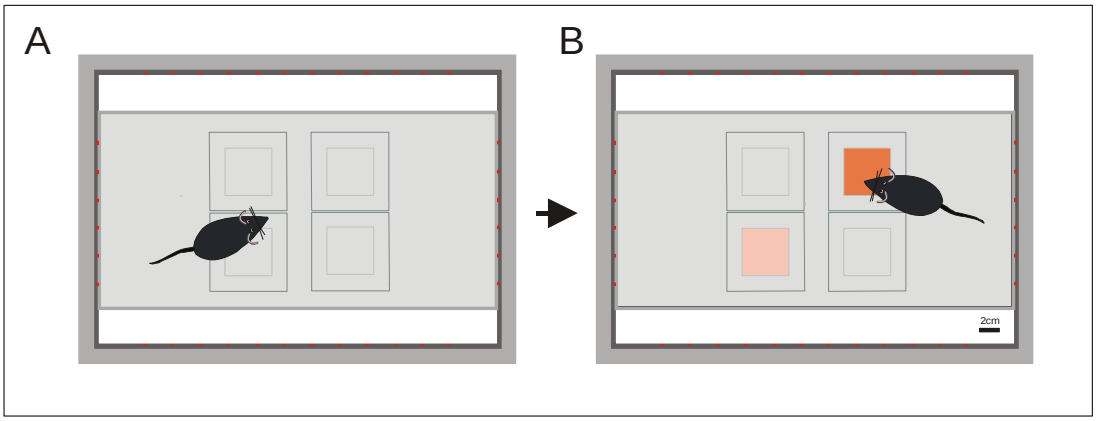

Figure 32 The tactile driven behavioural test based on natural sandpaper cues
Experimental design of the novel tactile acuity test for mice is shown. Mice were tested twice. **A)** In the negative experiment no tactile cues were inserted in neither of the positions. **B)** Rough and the smooth side of the sandpaper (roughness grade: 40) were placed randomly into two of four positions flush to the surface of the floor plate in the positive experiment. Cues were 50 x 50mm in size. Note that area quadrants including the surrounding area were calculated. Experiments were performed in complete darkness. The figure is drawn to scale.

C57BL/6N mice could easily discriminate between tactile cues and blank control inserts. (Fig. 33B and C left panel) This was already the case 30 minutes after introduction of the sandpaper cues. The mice showed a marked interest in the rough, but not in the smooth side, of the sandpaper as reflected by an increased time they spent in the vicinity of the rough sandpaper quadrant after inserting the cues (Fig. 33A), as well as in a longer distance they travelled within this quadrant (Fig. 33C). This behaviour may be a read-out of the different tactile quality of the rough structured sandpaper compared to its smooth side and the control insert.

SLP3$^{-/-}$ mice were also tested in the same task showing reduced interest in the rough side of the sandpaper as reflected in percentage of total distance they travelled (Fig. 33B) as well as in time they spent within the rough sandpaper quadrant (Fig. 33D). Therefore, and in contrast to C57BL/6N mice, SLP3$^{-/-}$ mice did not distinguish between the rough and the smooth side of the sandpaper as they explored both surfaces in almost the same manner.

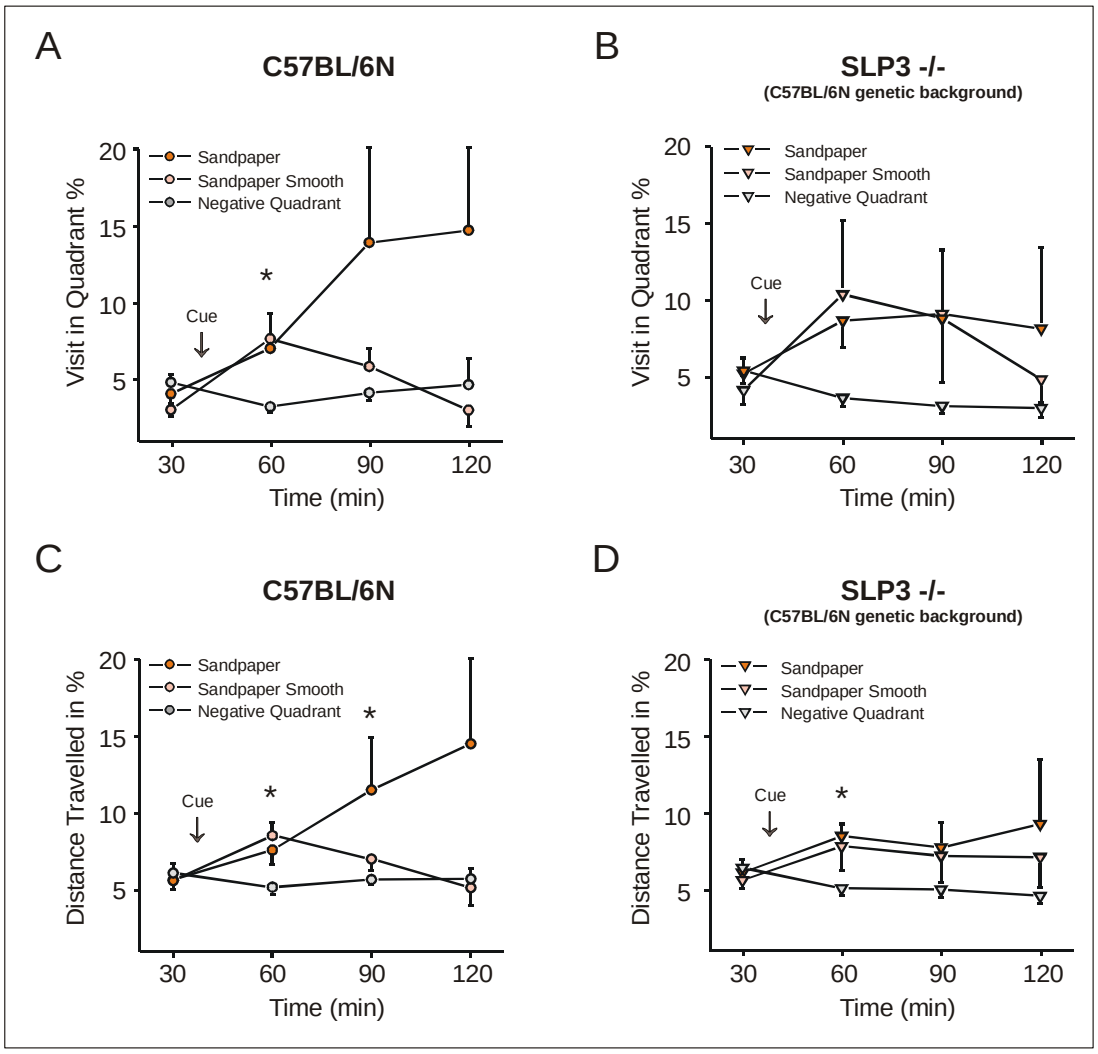

Figure 33 Behaviour of C57BL/6N and SLP3$^{-/-}$ mice on sandpaper cues
A-D) 12 adult mice per genotype were tested. Spatial location was analysed from "time visiting" the area quadrants (upper panel), activity behaviour from "distance travelled" (lower panel). Values are displayed as percentage of total. Percentage values for negative quadrants were calculated by averaging the four control inserts resulting from negative experiments. Note that C57BL/6N mice easily discriminated the smooth from the rough sandpaper cue **(A, C).** SLP3$^{-/-}$ mice did not distinguish between the two different surface cues **(B, D).** Error bars indicate s.e.m.

3.7.3 The grid-based quantitative tactile acuity test for mice

The sandpaper-based test described above has a number of disadvantages, for example the relative crudeness of commercially available sandpaper, but more importantly, the sandpaper has different olfactory qualities from the surrounding cage. These drawbacks prompted us to design a slightly different test using plastic inserts, made of the same material as the floor plate. These surface cues are grids that

vary in spatial frequency similar to tactile acuity cubes usually used in human touch tests (Van Boven and Johnson, 1994). In this new, now quantitative test, only two equivalent positions within the floor plate were chosen. They were symmetrically positioned along the middle axis of the box accommodating a putative tactile surface cue (plastic grid) at one position and a blank control insert exhibiting the same tactile property as the floor plate at the other position (Fig. 34).

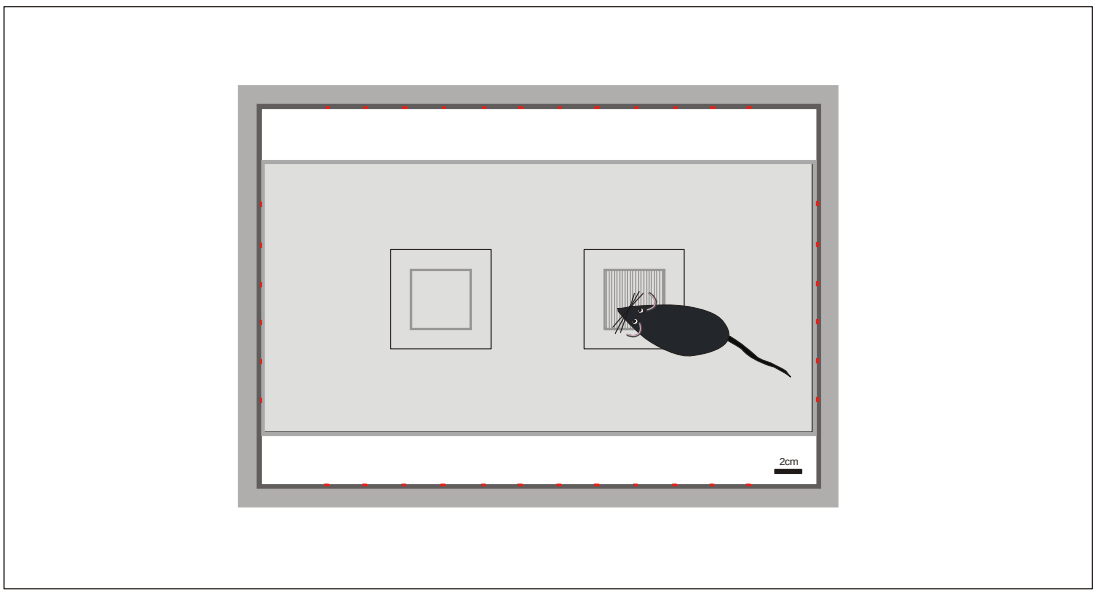

Figure 34 The tactile driven behavioural test based on Plexiglas cues with varying spatial frequency.
Two equivalent positions (42 x 42mm in size) were symmetrically arranged and placed along the middle axis of the box. Tactile surface cues were inserted into one while control inserts were placed into the other position, thus both positions could directly be compared. Area quadrants including the surrounding area of the surface were defined, which were 63mm^2 in size. Experiments were performed in complete darkness. The figure is drawn to scale.

In an initial experimental series, eight adult C57BL/6N mice were tested on seven different tactile surface cues with grid spacing extending from 250µm the narrowest up to 6mm the widest space. Including the control experiment, in which the mouse was confronted with two control inserts (indicated as control cue or “no-cue” respectively), each mouse was tested eight times within the test series completing a single experiment per day in which it was randomly confronted with only one of the grid cues. Activity/locomotion behaviour and spatial location within the surface area quadrant, which again included the surrounding area of the surface, was now directly comparable to the control quadrant at the opposite position containing the control insert (Fig. 34).

After 10 min habituation time one of the grid cues was introduced and the mice were monitored for a further 90 min in the box in complete dark environment. Locomotion behaviour and spatial location were analysed as percentage of total “distance travelled” or “ time visiting” within the individual quadrants. Values for each mouse are displayed as normalised ratios of surface cues to control inserts for the whole 90 min interval. Note that surface cue/control ratio =1.0 as long as the animal spent the same time in the vicinity of both, the surface cue as well as the control cue; surface cue/control ratio >1.0 in the case that the test animal spent more time in the vicinity of the surface cue than within the control quadrant; surface cue/control ratio <1.0 when the test animal spent less time in the vicinity of the surface cue compared to the control quadrant (Fig. 35A and B).

In the control experiment, C57BL/6N mice did not differentiate between both quadrants since “no-cue”/ control ratios spread evenly between 0.7 and 1.2 in terms of “distance travelled” (Fig. 35A) and between 0.8 and 1.7 for “time visiting” (Fig. 35B), i.e. average quotients were near one in both analyses (Fig. 35C). Exposing grid cues to the mice, the data indicate that C57BL/6N mice detected and responded to most of the grid cues. They showed a marked interest in surfaces with narrower spatial frequency (250µm up to 750µm) presumably because those surfaces are recognised as texture by mice. This effect was highly statistically significant in both cases, i.e. for the distance the mice travelled within the surface quadrants (paired T-test p=0.01(250µm), p=0.04 (500µm), p=0.007 (750µm), Fig. 35A) as well as for the time the mice spent in the vicinity of the cues (paired T-test p=0.03(250µm), p=0.03 (500µm), p=0.006 (750µm), Fig. 35B). On the other hand, C57BL/6N mice seem to avoid surfaces with a spatial frequency of 1mm or wider, although in most instances this was not statistically significant (Fig. 35C and D). Presumably, such surfaces are not perceived as texture elements by mice but possibly as edges or steps. (Note that the spatial frequency here is larger than a normal mouse toe.) C57BL/6N mice clearly distinguish 250µm spatial frequency from the control inserts indicating that the acuity threshold for detecting/ perceiving texture elements in mice must be below this spatial frequency. To show that this new quantitative test is reliable, experiments were repeated with another separate group of C57BL/6N mice under the same conditions. This second experimental trial produced broadly the same results for both locomotion and spatial analysis (data not shown).

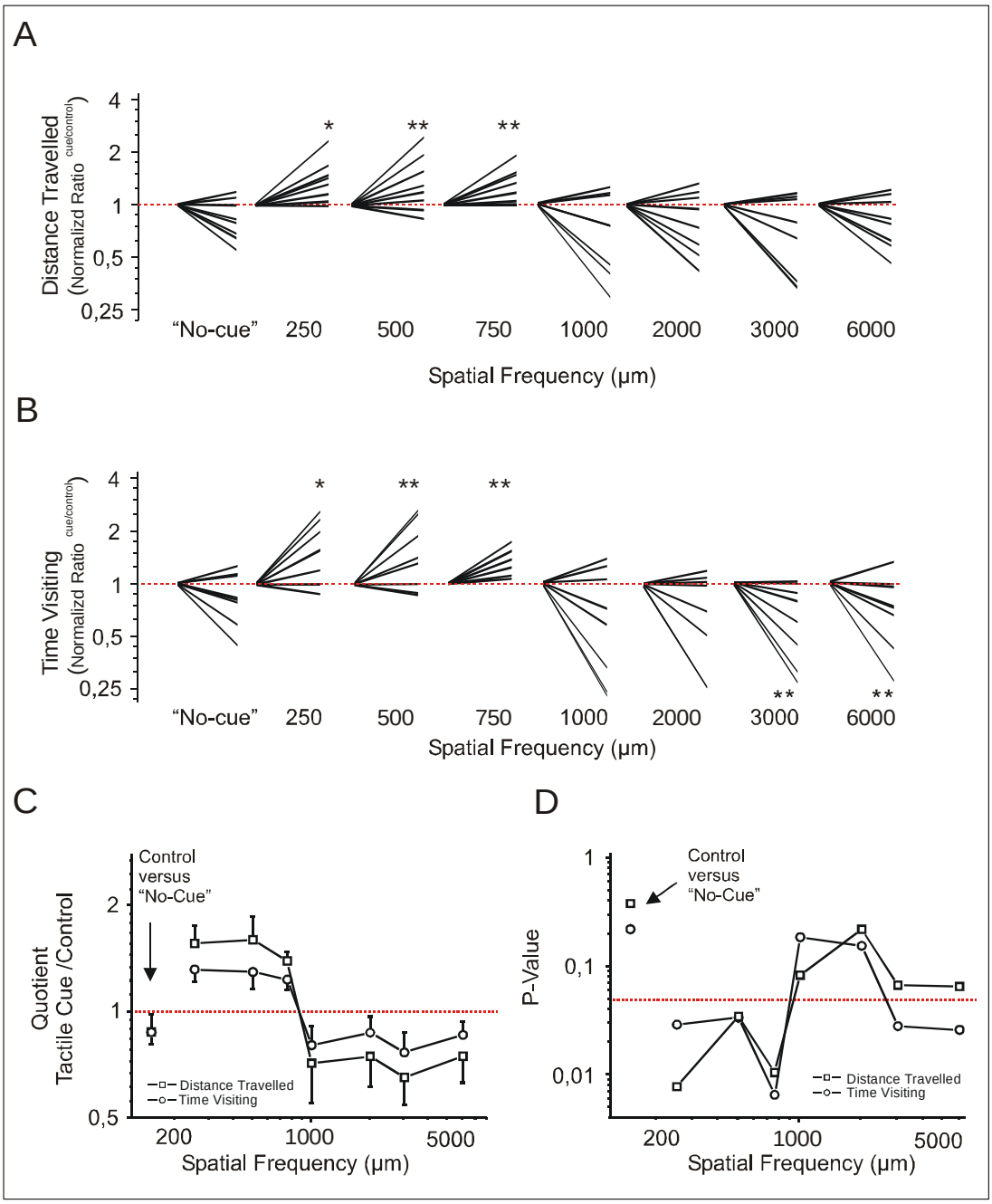

Figure 35 Behaviour of C57BL/6N mice on the quantitative grid-based tactile driven behavioural test

Eight adult C57BL/6N mice were examined on this quantitative test. **A, B)** Locomotion behaviour is displayed as "distance travelled" (A), spatial location is shown as "time visiting" (B) the area quadrant. Each line represents the individual surface cue/control ratio of one mouse. Note that C57BL/6N mice easily discriminated spatial frequencies of 250µm to 750µm as they developed a clear preference for these cues that was highly statistically significant (paired T-test **p<0.005). **C, D)** Average surface cue/ control quotients (C) or p-values (D) reflecting the statistical relevance (paired T-test) of the surface discrimination are displayed for each of the seven spatial frequencies for both analyses described above. Note that 1mm spatial frequency or wider were avoided by most of the C57BL/6N mice but this effect was only statistically significant were indicated (paired T-test **p<0.005). Error bars indicate s.e.m

3.7.4 Behaviour of SLP3$^{-/-}$ mice on the grid-based tactile acuity test

To further examine SLP3$^{-/-}$ mice using the new grid-based behavioural test 16 adult mice were tested as described above. Only those surfaces likely to be perceived as texture elements by C57BL/6N mice (250µm-750µm spatial frequency) were investigated. As explained before, C57BL/6N mice showed a marked interest in exploring all three grid cues. The preference they developed for these grids was statistically significant in terms of their activity/locomotion behaviour (paired T-test p=0.005(250µm), p=0.003 (500µm), p=0.001 (750µm), Fig. 36A, left panel) and also in terms of spatial resolution (paired T-test p=0.006(250µm), p=0.004 (500µm), p=0.0007 (750µm) Fig. 36B, left). Individually normalised surface cue/control ratios obtained from SLP3$^{-/-}$ mice on the other hand reflect a wider distribution, i.e. some of the mutants seemed to detect individual grid cues by travelling a wider distance within the surface cue area compared to the control quadrant. However, the majority of the SLP3$^{-/-}$ mice did not clearly differentiate between the control inserts and the grids, since on average surface cue/control ratios resulted in around one. Thus, in terms of the two finer grids SLP3$^{-/-}$ mice were on average not able to detect surface cues in a statistically significant manner concerning their activity/locomotion behaviour and also in terms of the time they spent in the vicinity of the grid cues (paired T-test p>0.05, Fig. 36A and B right panel). SLP3$^{-/-}$ mice developed an interest or preference that reached statistical significance only for the widest grid cue (750µm) tested but p-values were about 10 times higher than found in wild-type mice (paired T-test p=0.03 (time visiting) p=0.006 (distance travelled), Fig. 36B and C).

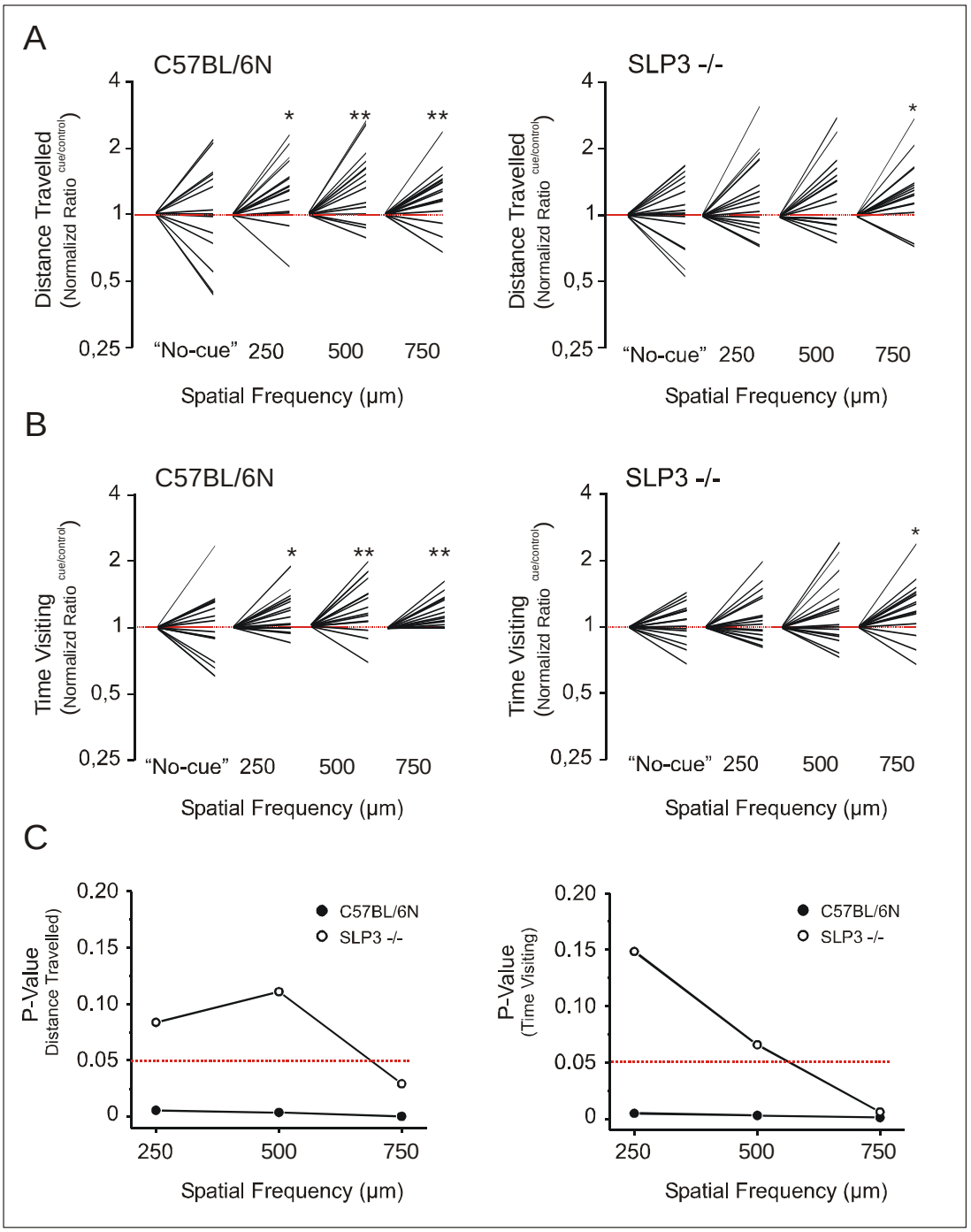

Figure 36 Behaviour of SLP3$^{-/-}$ mice on the grid-based tactile acuity test
Detection of three distinct grids (250-750µm spatial frequency), initially tested on wild-type mice, was examined for 16 adult C57BL/6N and SLP3$^{-/-}$ mice. **A, B)** Locomotion behaviour is displayed as "distance travelled" (upper panel). Spatial location is shown as "time visiting" the area quadrant (lower panel). Surface cue/control ratios were calculated (control set to 1.0) and shown as single lines for each of 16 mice (>1.0 more time on grid, <1.0 less time). **C)** P-values reflecting the statistical relevance (paired T-test) of discriminating grid cues are displayed for both analyses. Note that the majority of C57BL/6N mice spent more time in the vicinity of the cue for all grids tested, but SLP3$^{-/-}$ mice exhibited a significant preference only for the coarsest grid (paired T-test ** $p<0.005$, * $p<0.05$).

3.7.5 Performance of SLP3$^{-/-}$ mice on a rotorod treadmill

The somatosensory system is not only concerned with sensory information from the skin and viscera but also from joints or muscles. Proprioreceptors that provide the CNS with kinaesthetic information on muscle length and tension to control body movement and position are mechanoreceptors of either muscle spindle group Ia / II afferent fibres or the Golgi tendon organ. In order to investigate whether *slp3* deletion leads to impaired motor coordination in mice, SLP3$^{-/-}$ and C57BL/6N mice were tested on a rotorod treadmill using an accelerating program on this device. Eight mice per genotype were tested. The rotorod treadmill was accelerated from 5 to 65 rpm over a period of 120 seconds. When the mice were not able to perform any longer on the rotorod they fell off. Each mouse received three daily trials with 60sec resting time between the trials on 3 consecutive days. Although retention times recorded for SLP3$^{-/-}$ animals (43-47sec) in the first two experimental trials showed a reduced average performance of these animals compared to C57BL/6N mice (~52 sec) this was not statistically significant (unpaired T-test p=0.55 (trial one) p=0.70 (trial two), Fig. 37).

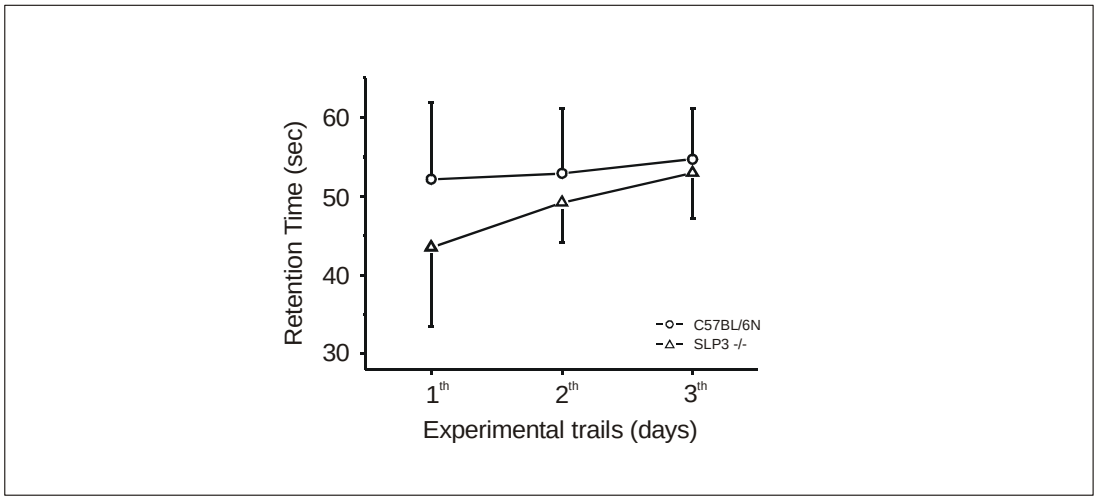

Figure 37 Mice performance on an accelerating rotorod treadmill
Effects of the loss of SLP3 on motor coordination were tested using a rotorod treadmill. The rotorod was accelerated from 5 to 65 rpm over a period of 120 seconds. The retention time until the mice fell off the rotorod was stopped with a timer that was connected with the floor plate. Tasks were repeated three times with 60sec resting time between the trials. Retention times on the rotating rod were compared between SLP3$^{-/-}$ and C57BL/6N mice. Eight mice per genotype were tested. The results indicate that rotorod performance is not different in SLP3$^{-/-}$ mice suggesting that the animals' motor coordination is not deficient.

Thus, the data suggest that motor coordination of SLP3$^{-/-}$ mice is not markedly deficient from C57BL/6N mice. Taking this into consideration the hypothesis is strengthened that the deficits in tactile discrimination observed in SLP3$^{-/-}$ mice are consistent with the deficits in mechanoreceptor function.

3.8 Paraoxonase genes and sensory mechanotransduction

In *C. elegans* not only MEC-2 but also MEC-6 is essential for the generation of a mechanoreceptor current in PML cells (O'Hagan et al., 2005). These neurones are required for behavioural responses to touch applied along the posterior wall of the worm's body (Chalfie et al., 1985). The closest mammalian homologue of MEC-6 in mammals is a protein called paraoxonase. At least three family members of the protein family are known in mammals: PON1, PON2 and PON3. To address the question of whether paraoxonase could be an interesting candidate molecule in vertebrate sensory mechanotransduction the following experiments were carried out.

3.8.1 Cloning of paraoxonase gene cDNAs

RT-PCR techniques were used to obtain a full-length cDNA clone from mouse DRG corresponding to the open reading frame of *pon2* (100% identical with the sequence published under GenBank accession number AAH62200) using gene specific oligonucleotide primers (Pon2-cDNA up and Pon2-cDNA low). *pon2* cDNA was cloned into pGEM-T Easy and subjected for sequencing before subcloning in the eukaryotic expression vector pTracerCMV.

The other two *paraoxonase* gene full-length cDNAs were obtained from EST clones (*pon1*: IMAG O064721Q2; *pon3*: IMAG B128764). The EST clone IMAG O064721Q2 (RZPD, Berlin) contained full-length cDNA corresponding to the ORF of mouse *pon1* (GenBank accession number AAH12706) showing 98.9 % identity to the published sequence. However, several nucleotide exchanges led to the following amino acid substitutions in the PON1 sequence: Glu61Gly, Leu305Pro, Arg306Gly, Ser335Phe. Since our *pon1* sequence was confirmed twice by sequencing of the EST clone inserts, these differences can only be explained by partial differences within the sequence of the EST clone itself.

Except for the first 15 base pairs the EST clone IMAG B128764 (RZPD, Berlin) contained full-length cDNA corresponding to mouse *pon3* (GenBank accession number AAH99416) showing 100 % identity to the published sequence. In order to

obtain *pon3* full-length cDNA a 5'oligonucleotide primer (Pon3-cDNAup) was designed that corresponds to the 5'end of the EST insert including the 15 missing base pairs of the *pon3* ORF. Using Pfu-polymerase, exhibiting 3'→5' exonuclease activity for providing low error rates (prove-reading), the complete ORF of *pon3* was amplified from this EST clone with "Pon3-cDNA up" and "Pon3-cDNA low". Subsequently *pon1* and *pon3* cDNAs were subcloned in pGEM-T Easy.

3.8.2 Expression of the different paraoxonase genes in sensory neurones

If paraoxonase like MEC-6 in *C. elegans* is involved in mechanotransduction in mammals it should be expressed in sensory neurones. To address this question expression of *paraoxonase* mRNA in mouse DRGs was examined using qPCR techniques. Therefore, two cDNA preparations were made from DRGs obtained from two C57BL/6N mice per preparation.

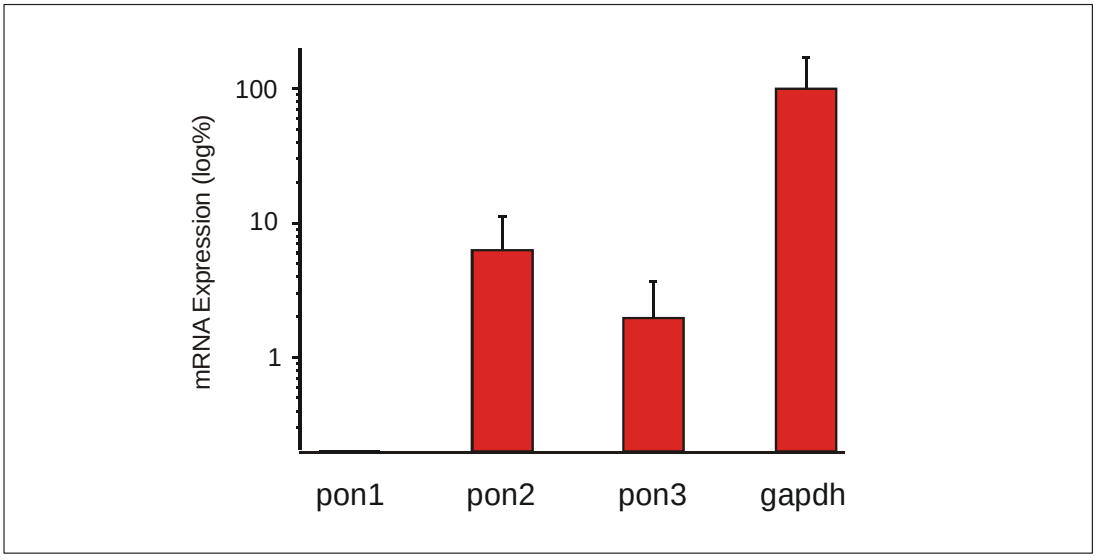

Figure 38 Expression of different *paraoxonase* mRNA transcripts in the DRG in mice
A qPCR was used to compare *pon1*, *pon2* and *pon3* mRNA expression. cDNA preparations were made from DRGs obtained from 2 animals per qPCR run, which were repeated twice. For mRNA quantification amplification rates of the target genes were compared to the housekeeping gene *gapdh*. The expression level of *pon2* mRNA was four times higher than that of *pon3* mRNA. *pon1* mRNA was not present in the DRG in mice. Error bars indicate s.e.m.

Pre-designed primer and probe sets offered by Applied Biosystems for the TaqMan Gene Expression Assays were chosen that correspond to the three mouse *paraoxonase* genes (*pon1*: TaqMan Expression Assay Mm00599936; *pon2*: TaqMan Expression Assay Mm00447159; *pon3*: TaqMan Expression Assay Mm00447161). Expression of all three possible mRNA transcripts was quantified as amplification rates of the target genes. Threshold cycles were compared to the housekeeping gene *gapdh* (TaqMan Expression Assay 99999915_g1).
Whereas *pon1* mRNA is not expressed in the DRG in mice, *pon3* and *pon2* mRNAs are present in sensory neurones, although the expression levels of the *pon2* and *pon3* transcripts are relatively low (*pon3*: 1.9% and *pon2*: 6.3%, Fig. 38) when normalised to the expression of *gapdh* mRNA (Fig. 38).

For generating *in situ* hybridisation probes, in order to test the specific expression pattern of pon2 mRNA on DRG sections, different regions within the individual *paraoxonase* genes were amplified by PCR using the following oligonucleotide primer pairs: ”PON1 in situ up and -low” (571bp; nucleotides 282>853 within its ORF); ”PON2 in situ up and -low” (480bp; nucleotides 6>468 within its ORF); ”PON3 in situ up and -low” (481bp; nucleotides 17>498 within its ORF). These amplification products were subcloned in pGEM-T Easy and DIG-labelled sense and antisense probes were made using the DIG RNA Labelling Kit (SP6/T7) from Roche. To confirm paraoxonase expression in sensory neurones these probes were used in *in situ* hybridisation experiments on DRG cryosections obtained from C57BL/6N mice showing that *pon2* mRNA was the predominant transcripts expressed in all sensory neurones of the DRG in mice regardless whether they have large or small size somata (Fig. 39). Thus, *pon2* was selected for further experimental studies.

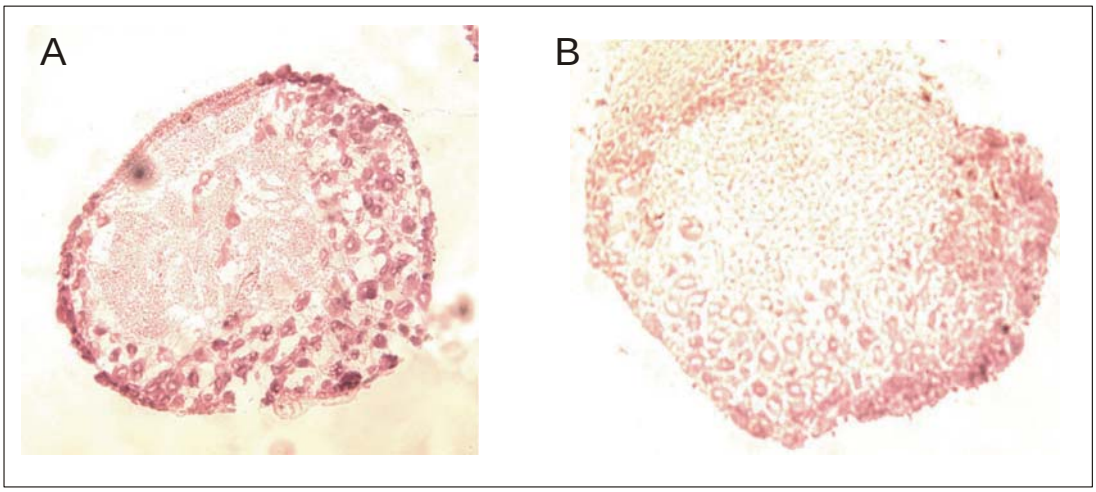

Figure 39 Expression of *pon2* mRNA in the DRG in mice
A DIG-labelled RNA probe corresponding to a unique sequence (~500bp) within *pon2* was used for *in situ* hybridisation on DRG sections. **A)** Darkly stained cells express *pon2* mRNA. Neurones of all sizes express *pon2* mRNA. There is no expression of *pon2* mRNA in axon tracts. **B)** *In situ* hybridisation experiments using sense controls revealed no staining in mouse DRG neurones.

3.8.3 Analysis of the PON2 sequence and secondary structure using bioinformatic tools

Experiments performed in *C. elegans* suggest that the paraoxonase homologue MEC-6 is a membrane bound protein extending its C-terminus into the extracellular space (Chelur et al., 2002). Biophysical analysis tools revealed that PON2 in mice is presumably an extracellular protein (see also http://www.expasy.ch/tools/) but that the protein probably does not exhibit a classical transmembrane domain since amongst others the TMHMM biophysical tool (Moller et al., 2001) did not compute any transmembrane helicies from the peptide sequence. However, PON2 seems to contain a signal peptide sequence at the N-terminus of the transcript, as the SignalP biophysical tool (Bendtsen et al., 2004) (Nielsen, 1997) predicted a cleavage site that is most likely located between positions 23 and 24 of the precursor peptide. Using the big-PI-predictor tool (Eisenhaber et al., 1999; Eisenhaber B, 1998) and the GDPI biophysical tool (Kronegg, 1999) it turned out that although the C-terminal hydrophobic area might be to short within the PON2 precursor peptide there is a potential GPI modification site found at position 330 of the peptide. In addition, the protein exhibits at least three potential asparagines predicted to be N-glycosylated.

3.8.4 Subcellular localisation of PON2 in a heterologous expression system

If PON2 is bound to the cell membrane via a GPI-anchor the insertion of a FLAG- or MYC-tag attached to the C-or N-terminus of the protein would potentially disrupt the membrane anchoring since no GPI anchor for PON2 could be synthesised. Thus, using the ExSite PCR-based site directed mutagenesis kit an internal FLAG-tag was inserted into mouse *pon2* cDNA at position 912 (ATG (Met) start codon = position 1) in frame with the protein sequence previously cloned in the mammalian expression vector pTracerCMV. Recombinant PON2 expression was then produced by a lipofectamine-based transfection of HEK293 with this mammalian *pon2* expression construct, called PON2B1. Western blot experiments were performed to test different protein fractions of the transfected HEK293 cell lysate for PON2 abundance by immunostaining using anti-FLAG M2 primary antibodies. Although M2 antibodies also weakly labelled unspecific protein bands in the Triton X-100 soluble membrane fraction, in both PON2 transfected as well as non-transfected (i.e. cells here were transfected with a pTracer-CMV control plasmid) HEK293 cells the same antibody detected a clear protein band of ~45kDa that was only found in PON2 transfected HEK293 cells. Human PON1 and PON3 are known to be secretory proteins, moreover tightly bound to HDL particles (Blatter et al., 1993; Kelso et al., 1994; Reddy et al., 2001). However, there was no 45kDa immunoreactive band, labelled by M2 antibodies, observed in the medium of *pon2* transfected HEK293 cells. No 45kDa immunoreactive bands could be detected in the soluble lysate fractions of *pon2* transfected or non-transfected HEK 293 cells using anti-FLAG antibodies (Fig 39). This result is consistent with the findings of Ng and colleagues who detected PON2 protein in the plasma membrane fraction of HMEC extracts (Ng et al., 2001).

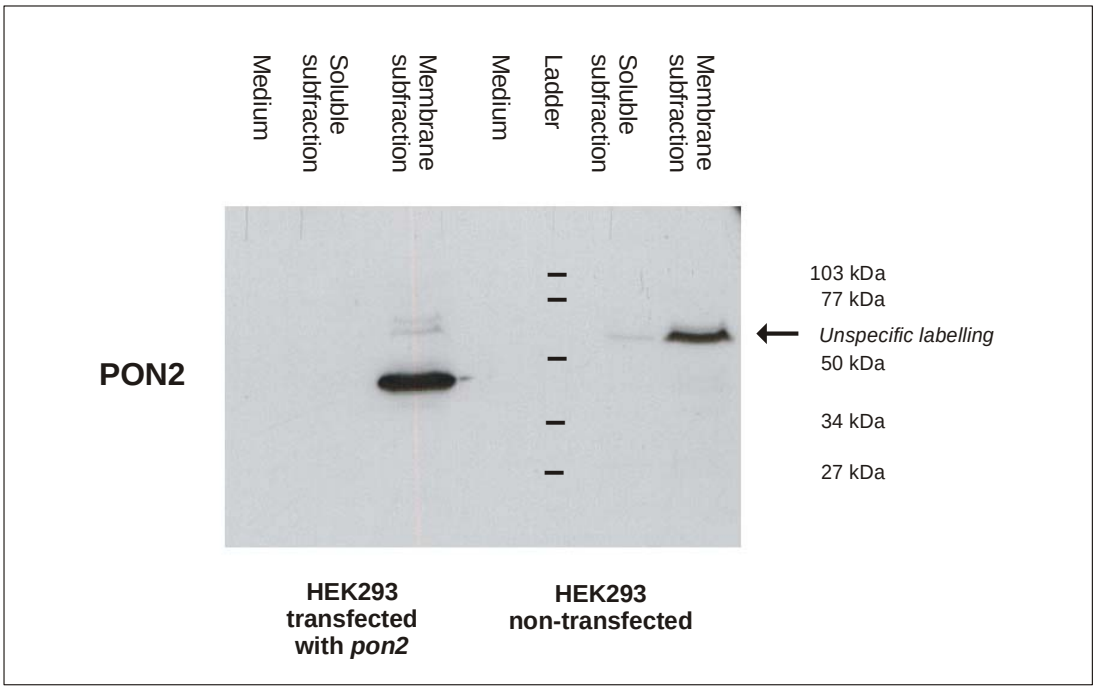

Figure 40 Western blot detecting PON2 in transfected HEK293 cells
Proteins were extracted from HEK293 cells transiently transfected with *pon2* that exhibits an internal FLAG-epitope in frame with the mouse PON2 protein. Ultracentrifugal fractions were separated under reducing conditions by SDS-PAGE before blotting them onto a nitrocellulose membrane. PON2 was detected in the Triton X-100 soluble membrane fraction using the anti-FLAG primary antibodies (M2).

3.8.5 Release of PON2 from plasma membranes by PI-PLC

Glycosylphosphatidylinositol (GPI) is a complex glycolipid that acts as a membrane anchor for many cell-surface proteins. Synthesised in the endoplasmatic reticulum, GPI is transported to the cell membrane and transferred to the C-terminus of a protein that exhibits a GPI attachment signal peptide before to be transported to the cell membrane (reviewed by (Low and Saltiel, 1988). To address the question of whether PON2 could be a GPI-anchored protein involved in mechanotransduction PI-PLC cleavage experiments were carried out. Therefore, HEK293 cells were again transiently transfected with the mammalian *pon2* expression construct PON2B1. Phosphatidylinositol phospholipase C from *Bacillus thuringiensis*, which specifically hydrolyses the phophsodiester bond of phosphatidylinositol, was used to test the transfected cells for a possible GPI-anchoring of the protein. If indeed PON2 would

be attached to the outer surface of the cell membrane via a GPI-anchor, it should be cleaved by PI-PLC and released from plasma membranes.

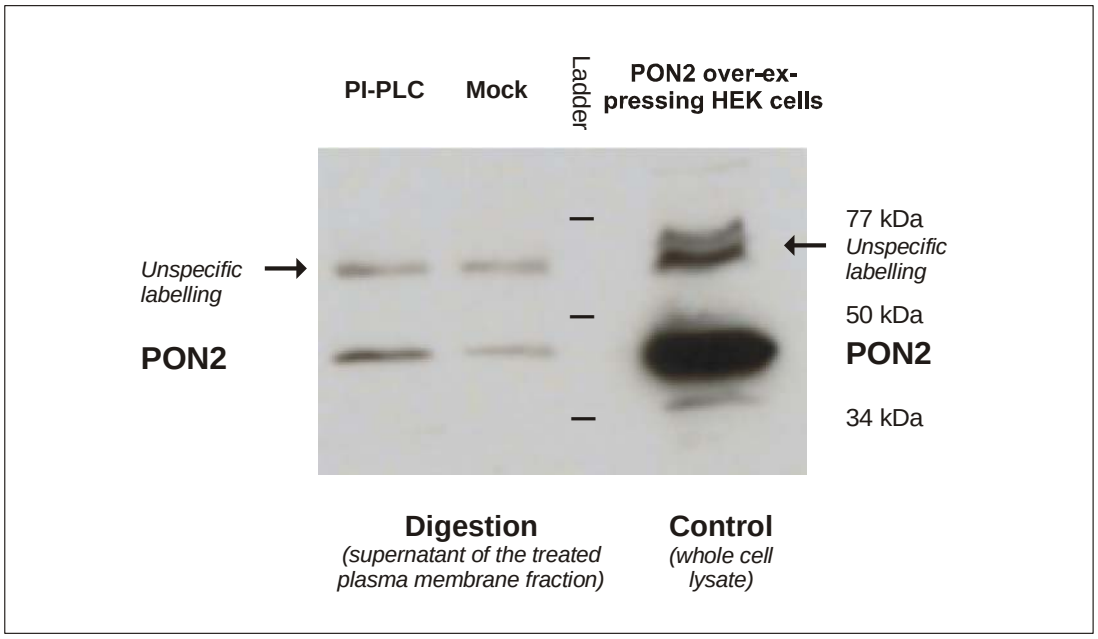

Figure 41 Release of PON2 from plasma membranes by PI-PLC
HEK293 cells were transiently transfected with a mammalian *pon2* expression construct exhibiting an internal FLAG-tag for later on detection of the protein. The release of PON2 from plasma membranes following either PI-PLC or mock digestion was tested by immunostaining using M2 primary antibodies. Note that labelling intensity is stronger in the PI-PLC digestion compared to the mock digestion using inactivated PI-PLC enzyme.

Thirty-six hours after transfection plasma membranes fractions containing the same concentration of total protein were isolated and used for either PI-PLC or mock digestion to test for the presences of PON2. Following PI-PLC digestion plasma membranes were pelleted and supernatants were analysed for PON2 release by immunostaining with M2 primary antibodies following SDS-PAGE and Western blotting.

Results show a clear release of PON2 from plasma membranes, since the antibody labelled a ~45kDa protein band in western blotting when cells were treated with PI-PLC enzyme (Fig. 40). In the mock digestion a protein band of the same size was detected but the labelling intensity was much lower compared to the PI-PLC digestion of PON2 transfected HEK293 cells (Fig.37). However, although the experiments were repeated twice a 45kDa immunoreactive band was again also detected in the mock digestion and this possibly arose from experimental conditions

of the cleavage procedure itself indicating that the digestion protocol has to be evaluated and to be improved. However, the labelling intensity of the PON2 band is much higher compared to the PI-PLC mock digestion (Fig. 37).